Searching for the QCD Critical End Point through (Net-)Proton Fluctuation at RHIC

Yige Huang

Institute of Modern Physics, CAS

2025/10/26 - Guilin - QPT2025

Outline

1. *Phase Transition & Critical Point*
2. *RHIC-STAR Experiment*
3. *Fluctuation Measurements*
4. *Selected Results*
5. *Summary & Outlook*

Phase Transition & Critical Point

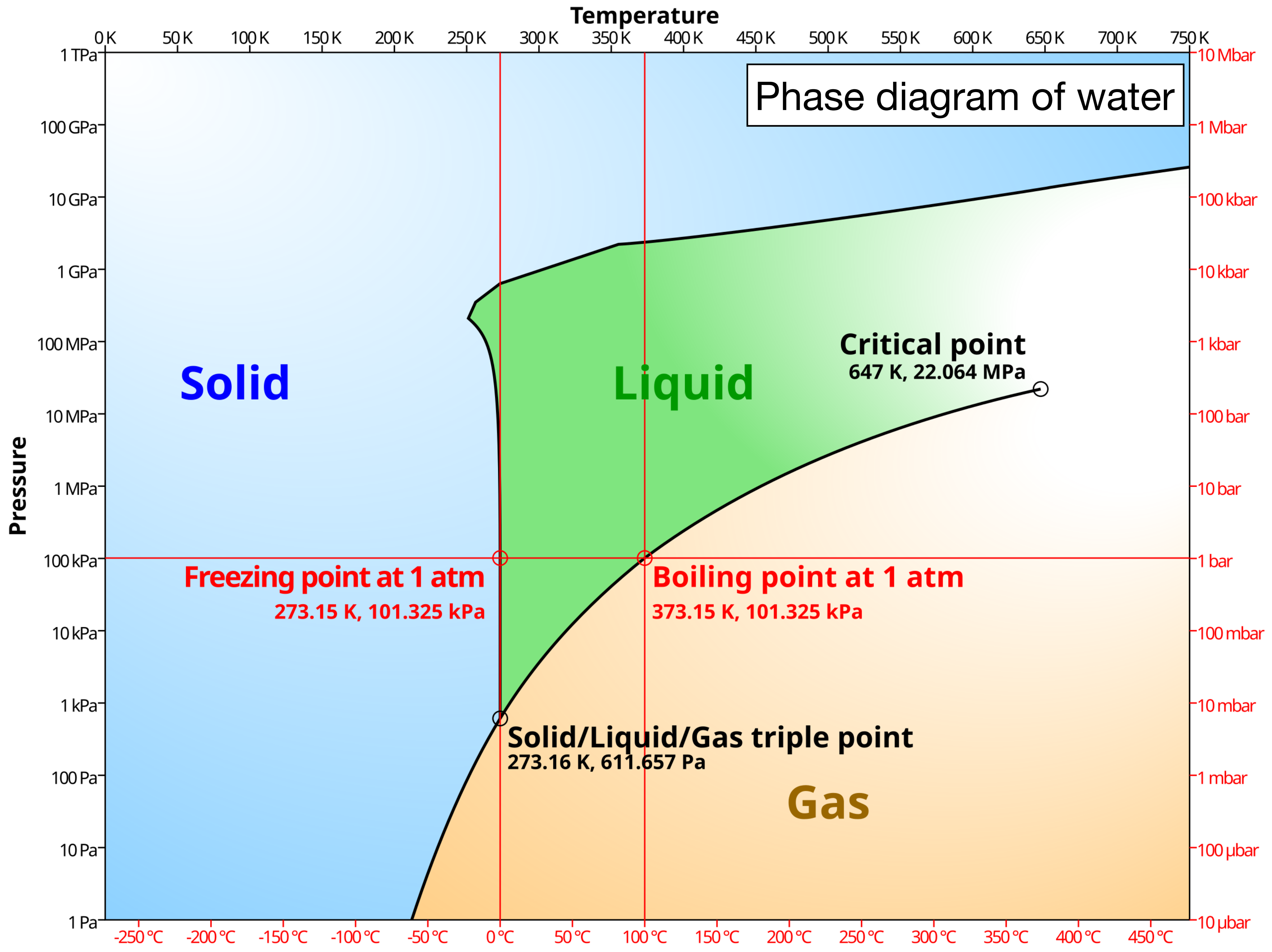

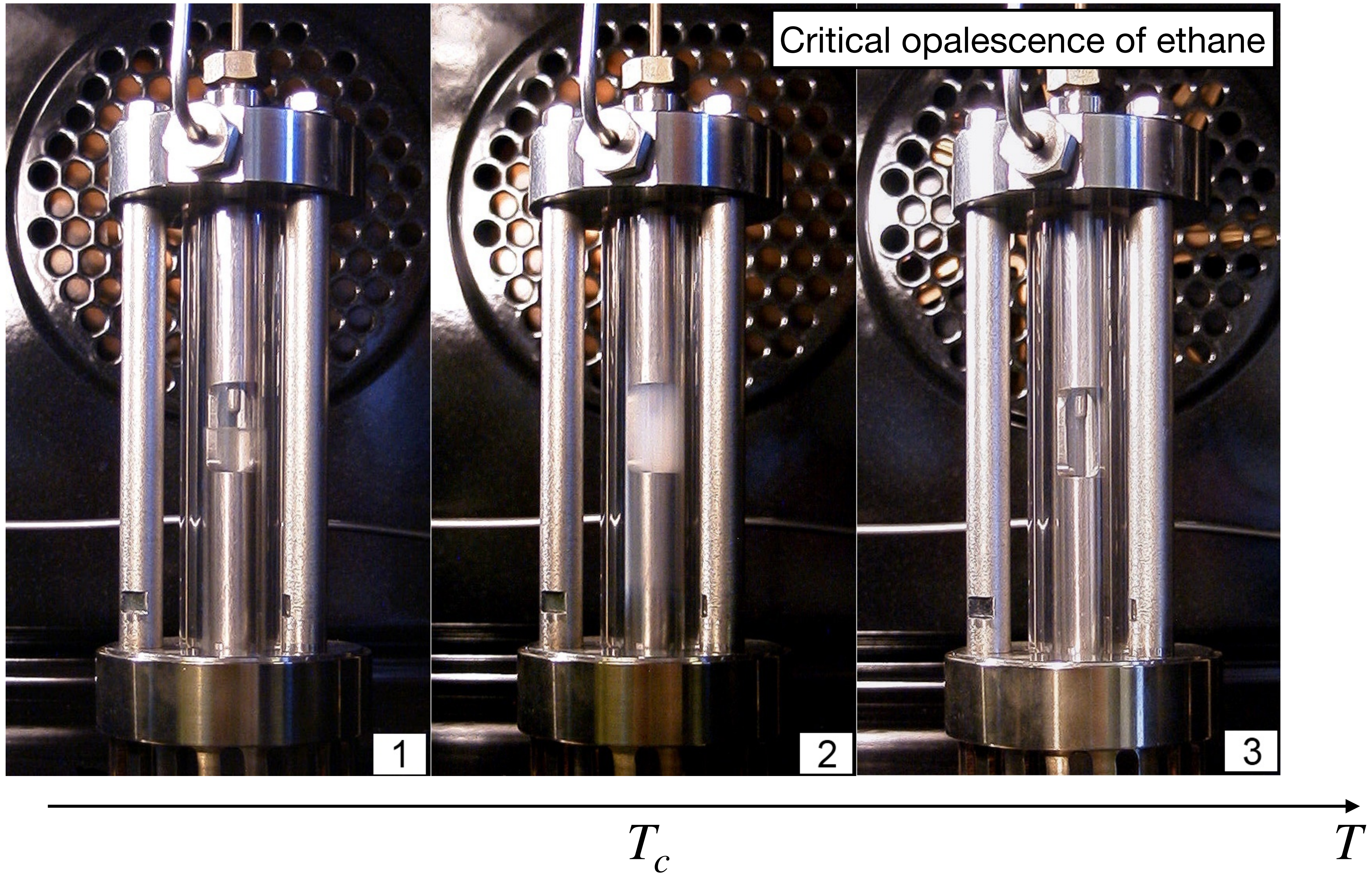

1. Phase transitions can be illustrated with the water phase diagram, including a critical point;
2. Near the critical point, diverging correlation length and enhanced density fluctuations lead to critical opalescence (ethane example).

Phase Transition & Critical Point

Y. Aoki, et al: Nature 443 675 (2006)
HotQCD: PRD 85 054503 (2012)
X. Luo, et al: Particles 3 278 (2020)

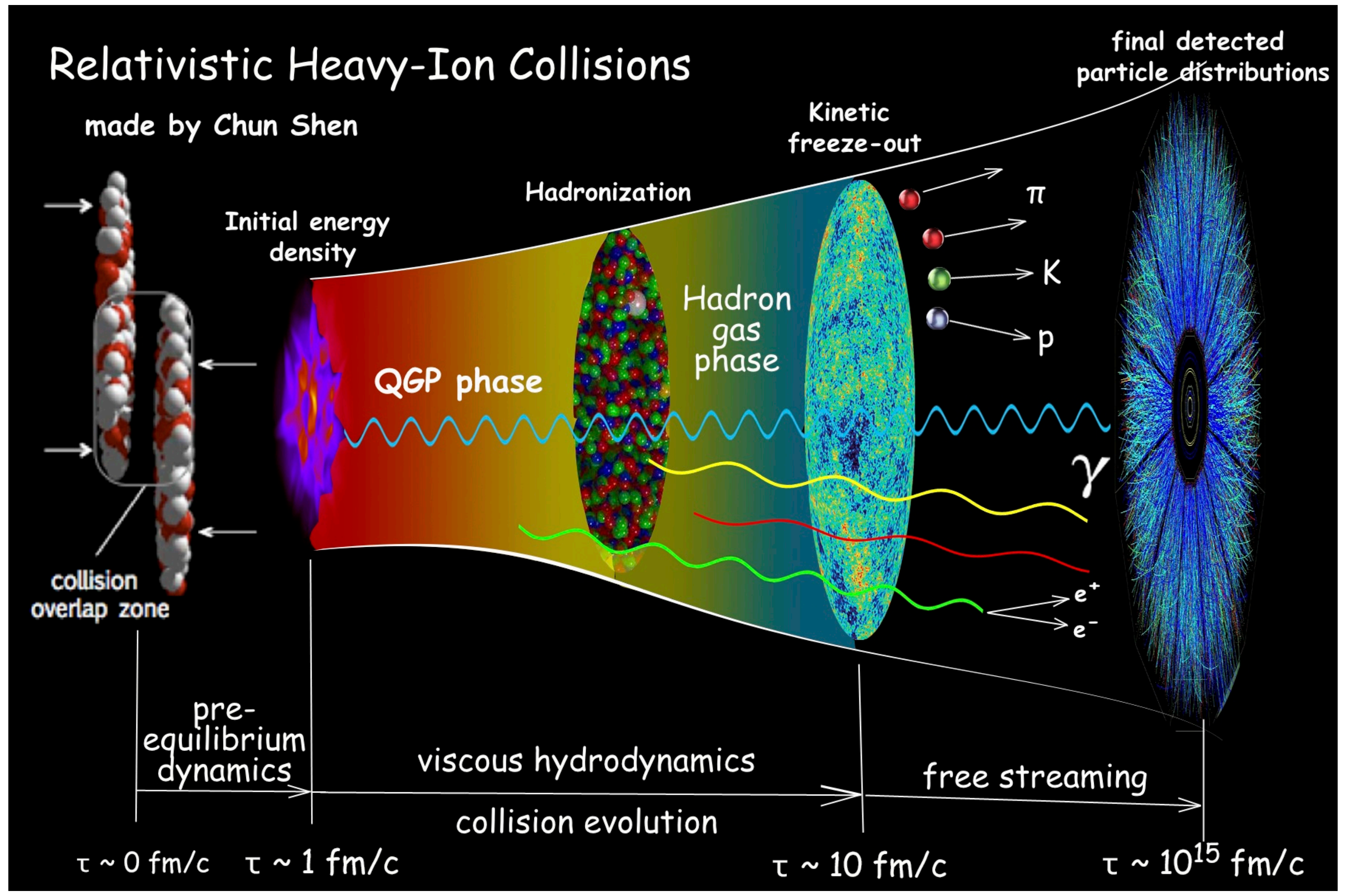

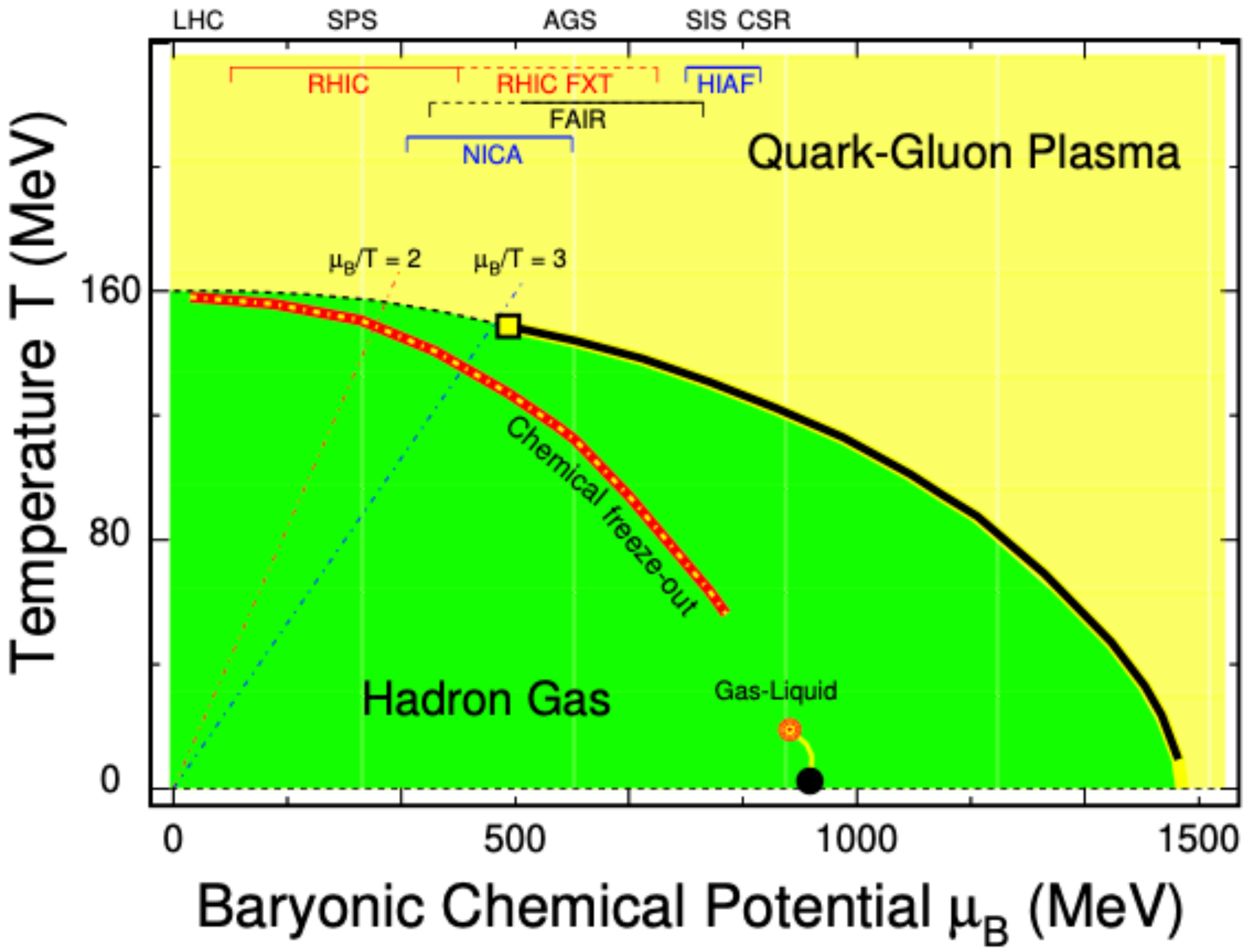

- Lattice QCD: at $\mu_B \sim 0$ MeV, smooth crossover;
- Large μ_B: first-order phase transition and a critical point?

1. Hadronic matter at extremely high temperature and density turns into quark-gluon plasma (QGP);
2. QCD phase diagram: to study the transition between hadronic matter and QGP;
3. Experiments probe the phase diagram along the chemical freeze-out curve.

Phase Transition & Critical Point

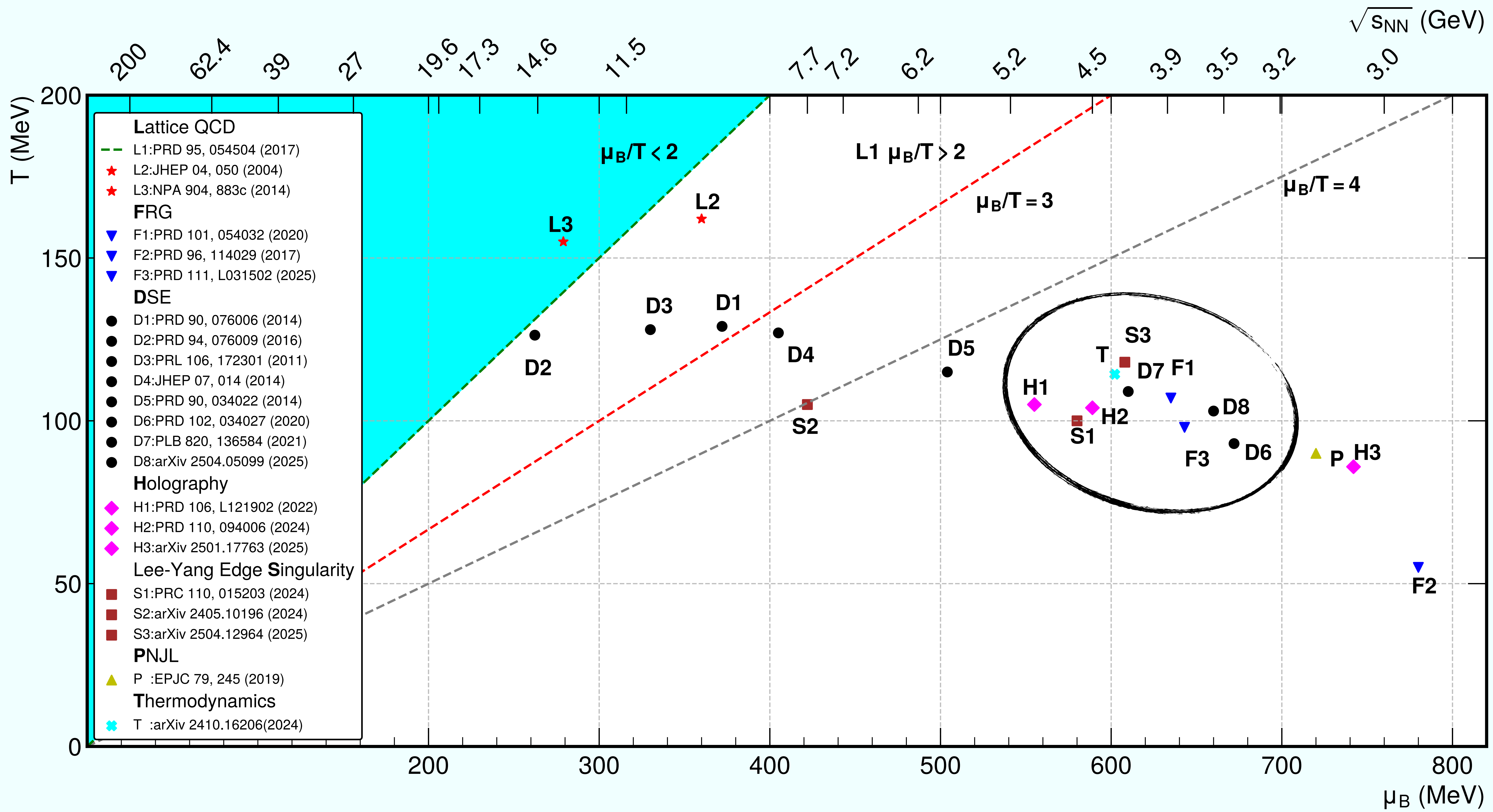

1. Extensive theoretical efforts have been devoted to locating the critical point;
2. Predictions in recent years cluster around μ_B ~ 600 MeV;
3. Experimental confirmation is still required.

STAR Detector System

BES-II Upgrades

RHIC Beam Energy Scan (BES)

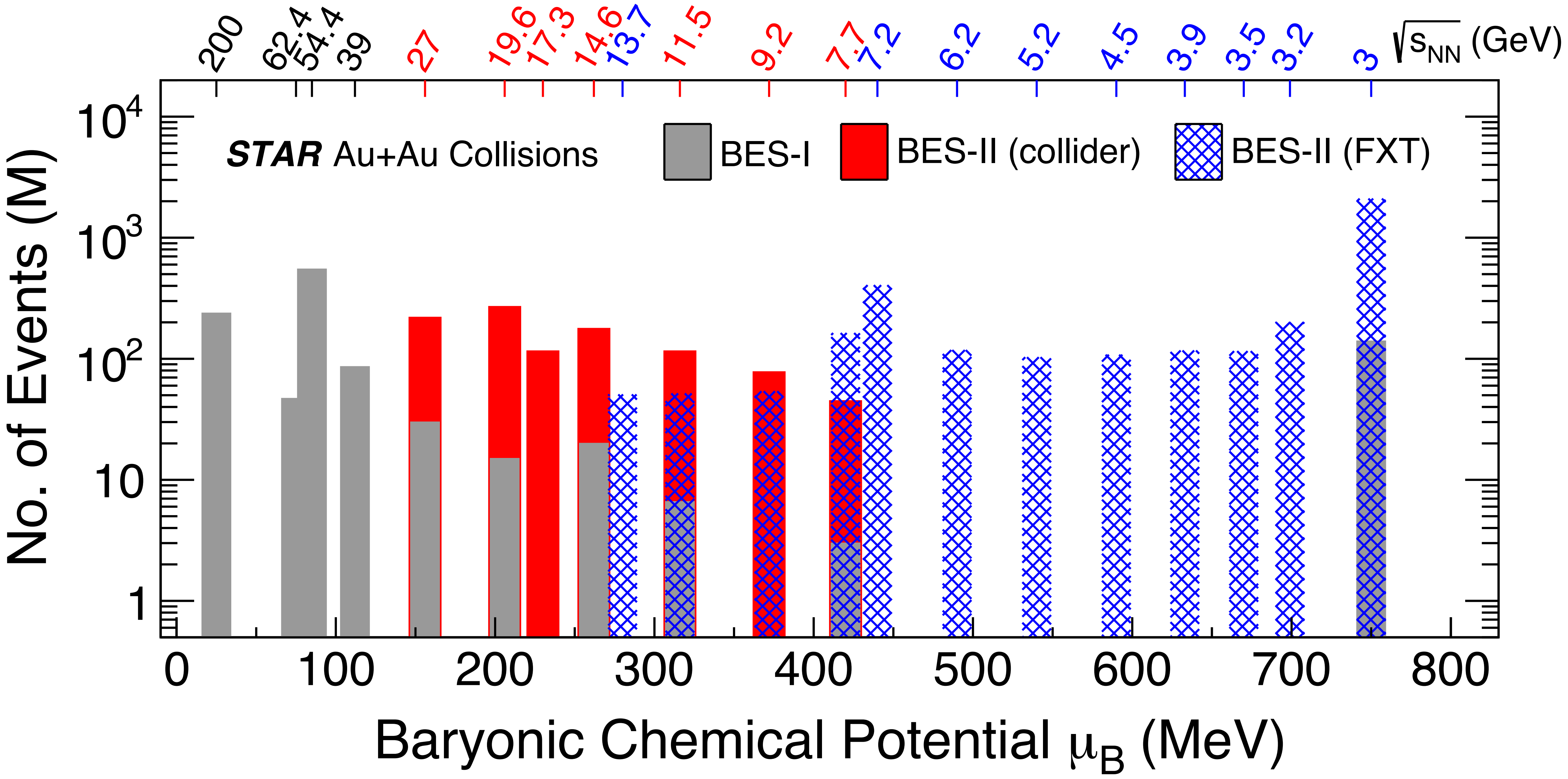

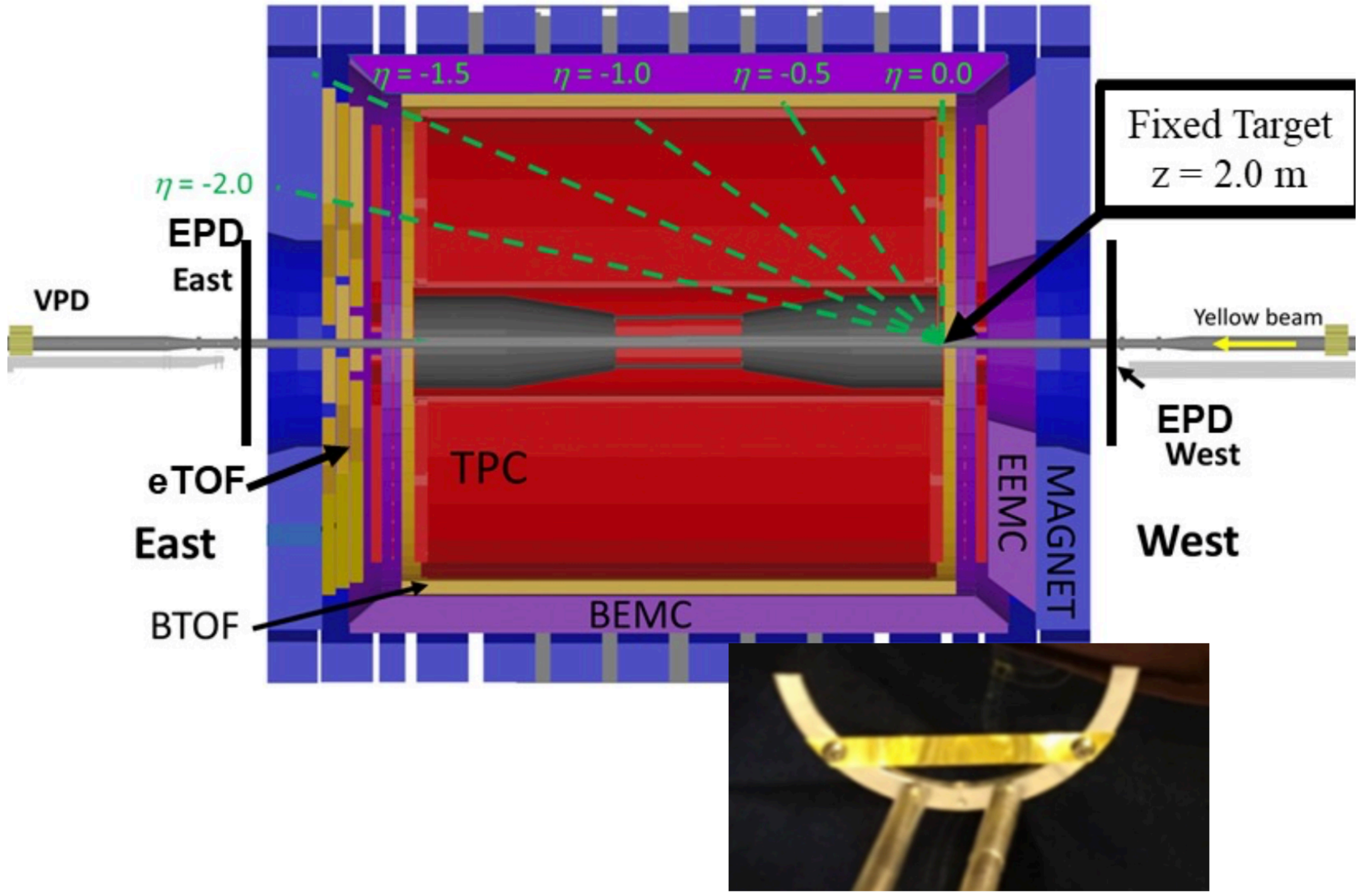

1. BES-I (2010–2014): Au+Au at 7.7 -> 200 GeV
2. BES-II (2018-2021): Au+Au at
   1) Collider mode: 7.7, 9.2, 11.5, 14.6, 17.3, 19.6, 27 GeV
   2) Fixed-target mode: **3.0**, **3.2**, **3.5**, **3.9**, **4.5**, 5.2, 6.2, ...,13.7 GeV
3. μ_B coverage : 25 — 760 MeV

Detailed Discussion: see ***Yu Zhang*** @ Oct. 25

Beam Energy Scan Phase-II (COL Mode)

Particle Identification

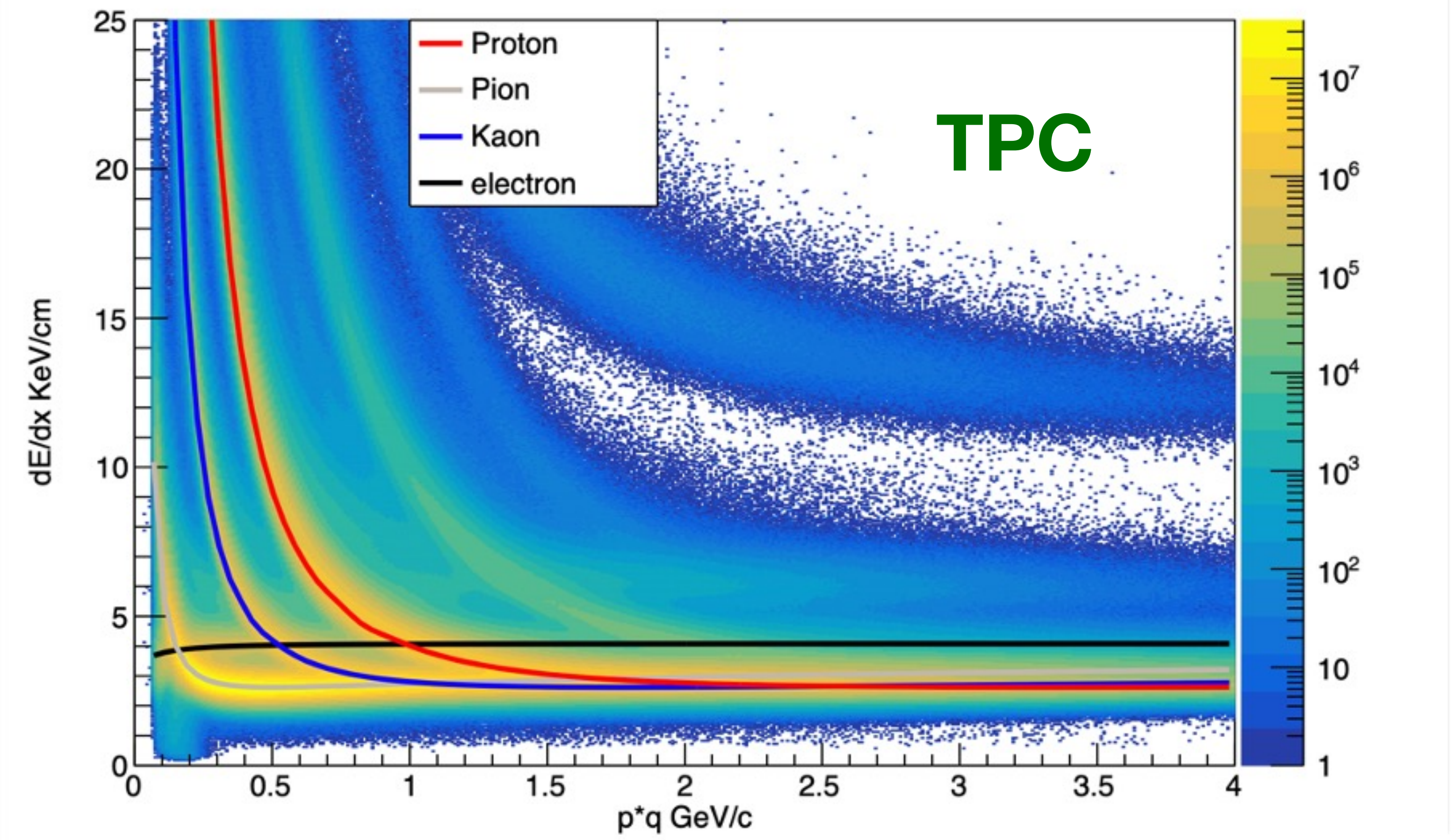

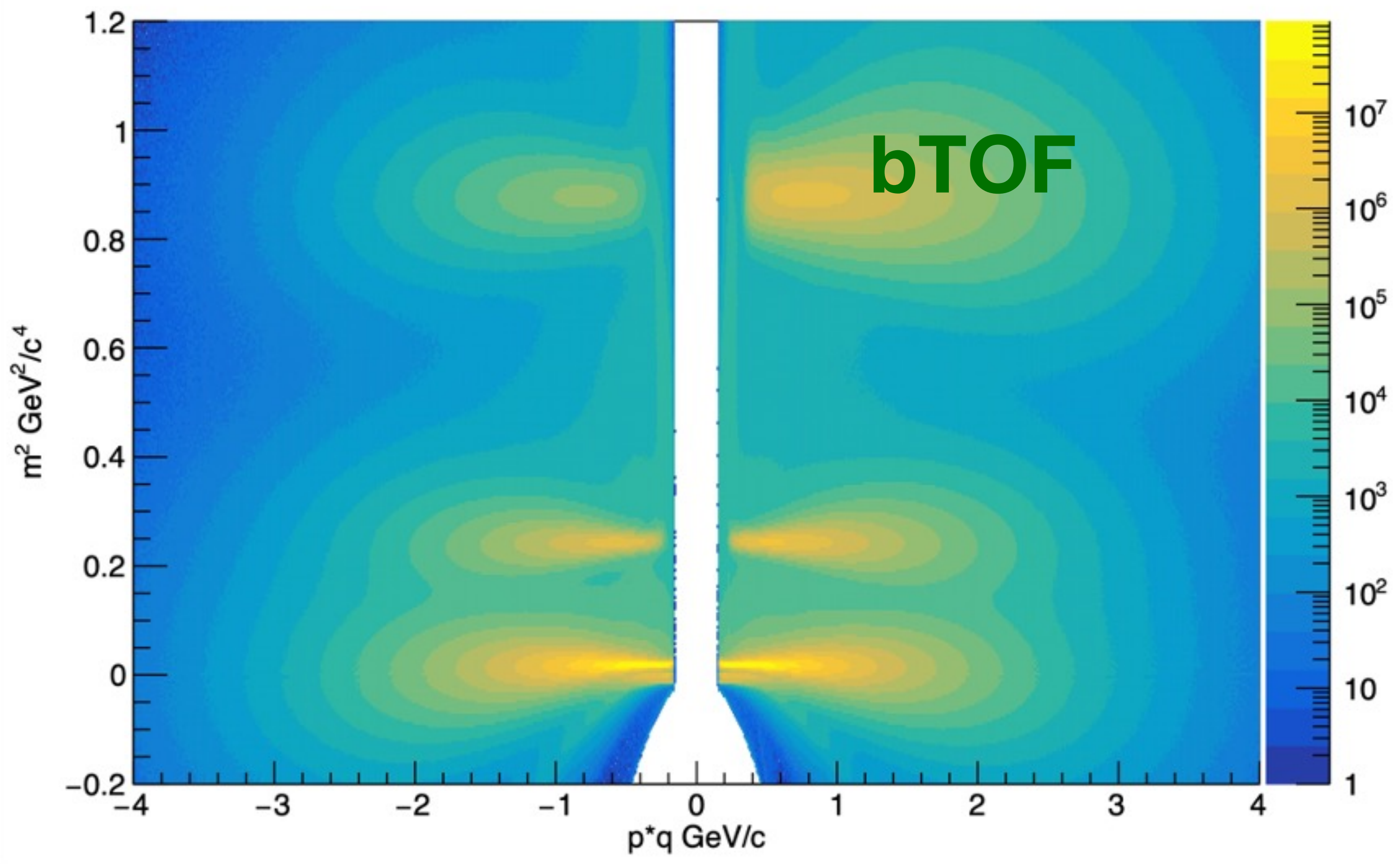

Collider Runs (COL)			Fixed-Target Runs (FXT)		
$\sqrt{s_{NN}}$ (GeV)	#Events	μ_B	$\sqrt{s_{NN}}$ (GeV)	#Events	μ_B
200	380 M	25 MeV	13.7 (100)	50 M	280 MeV
62.4	46 M	75 MeV	11.5 (70)	50 M	320 MeV
54.4	1200 M	85 MeV	9.2 (44.5)	50 M	370 MeV
39	86 M	112 MeV	7.7 (31.2)	260 M	420 MeV
27	585 M	156 MeV	7.2 (26.5)	470 M	440 MeV
19.6	595 M	206 MeV	6.2 (19.5)	120 M	490 MeV
17.3	256 M	230 MeV	5.2 (13.5)	100 M	540 MeV
14.6	340 M	262 MeV	4.5 (9.8)	110 M	590 MeV
11.5	57 M	316 MeV	3.9 (7.3)	120 M	633 MeV
9.2	160 M	372 MeV	3.5 (5.75)	120 M	670 MeV
7.7	104 M	420 MeV	3.2 (4.59)	200 M	699 MeV
			3.0 (3.85)	260 + 2000 M	760 MeV

Proton Acceptance

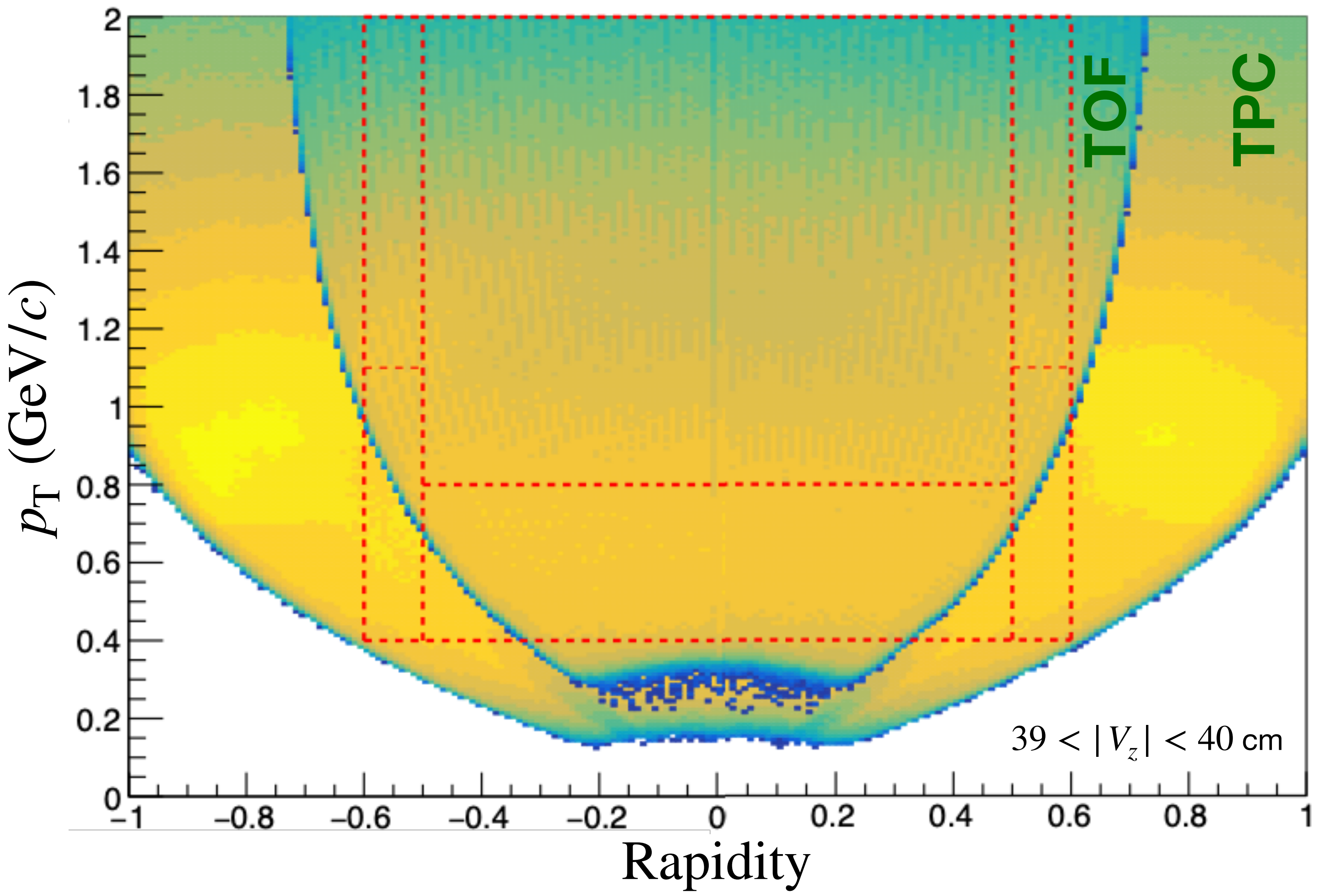

Examples from Au+Au collisions at $\sqrt{s_{NN}} = 19.6$ GeV

Centrality Definition

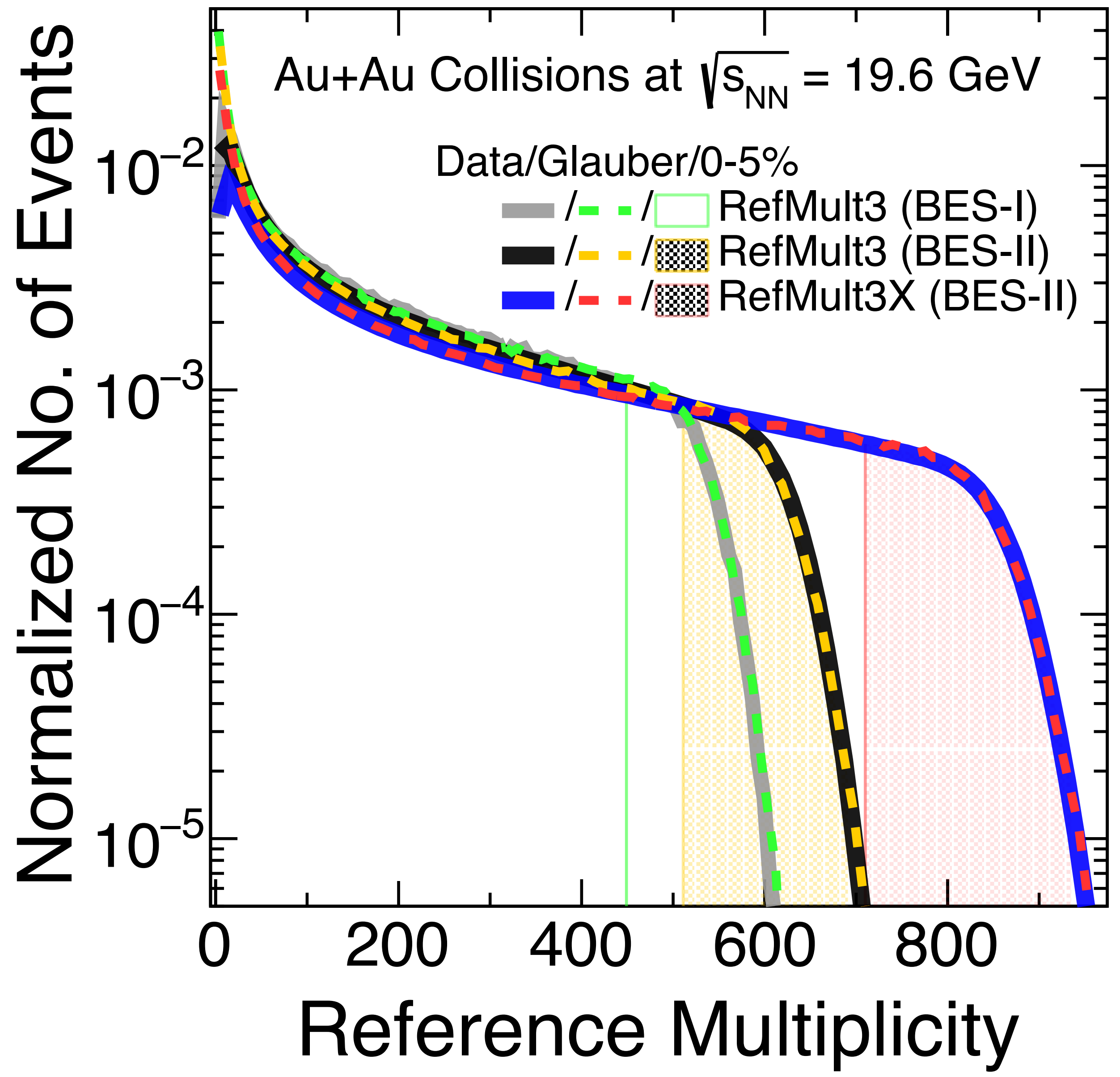

1. Excellent PID ensures high proton purity (> 95%);
2. Wide and uniform acceptance;
3. RefMult3(X): multiplicity of charged particles excluding protons (to avoid self-correlation)

Beam Energy Scan Phase-II (FXT Mode)

Particle Identification (Additional to TPC & bTOF)

- From CBM-TOF group
- Provides precision PID over $1.55<\eta<2.2$
- Collected data for FXT runs

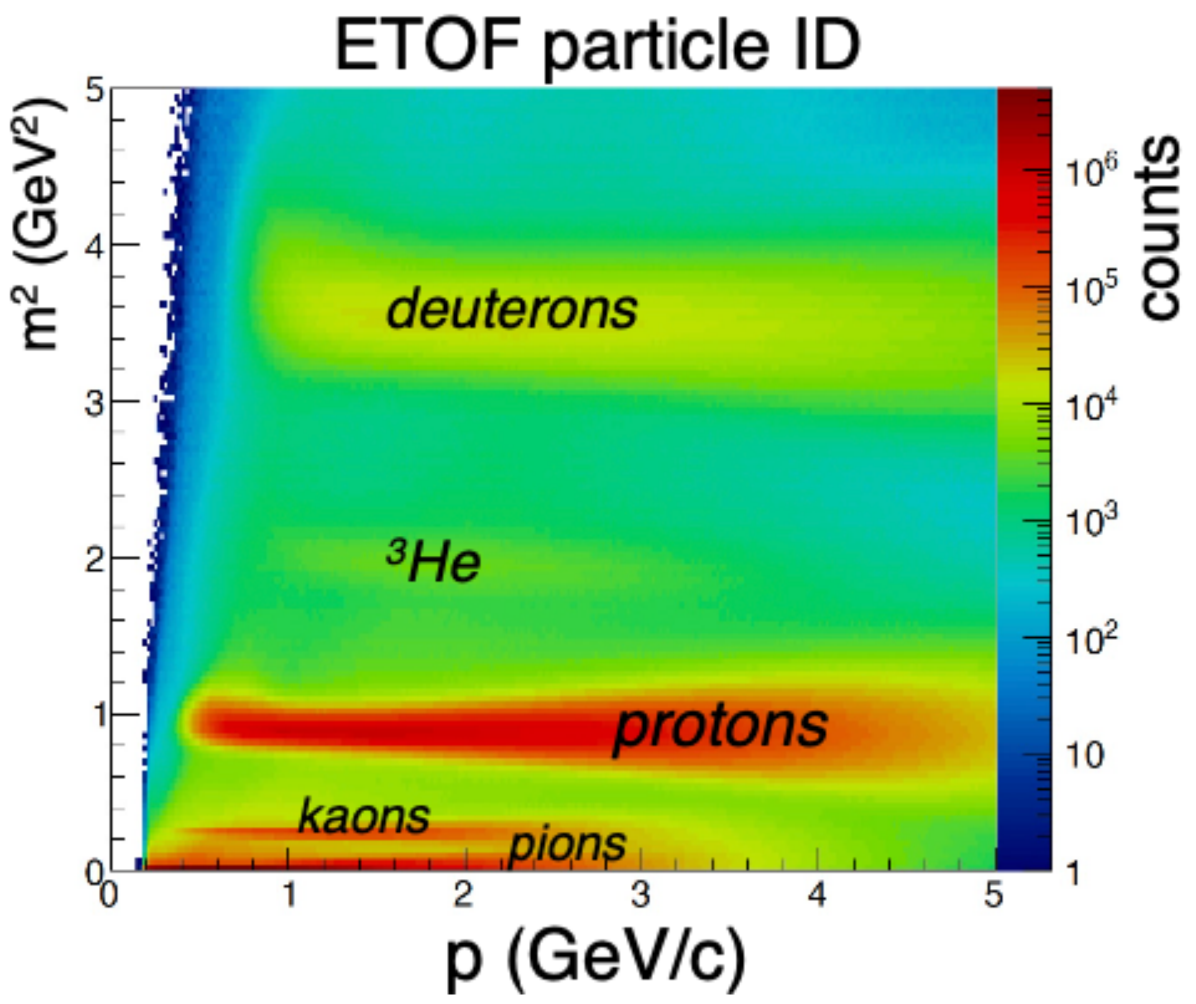

Collider Runs (COL)			Fixed-Target Runs (FXT)		
$\sqrt{s_{NN}}$ (GeV)	#Events	μ_B	$\sqrt{s_{NN}}$ (GeV)	#Events	μ_B
200	380 M	25 MeV	13.7 (100)	50 M	280 MeV
62.4	46 M	75 MeV	11.5 (70)	50 M	320 MeV
54.4	1200 M	85 MeV	9.2 (44.5)	50 M	370 MeV
39	86 M	112 MeV	7.7 (31.2)	260 M	420 MeV
27	585 M	156 MeV	7.2 (26.5)	470 M	440 MeV
19.6	595 M	206 MeV	6.2 (19.5)	120 M	490 MeV
17.3	256 M	230 MeV	5.2 (13.5)	100 M	540 MeV
14.6	340 M	262 MeV	4.5 (9.8)	110 M	590 MeV
11.5	57 M	316 MeV	3.9 (7.3)	120 M	633 MeV
9.2	160 M	372 MeV	3.5 (5.75)	120 M	670 MeV
7.7	104 M	420 MeV	3.2 (4.59)	200 M	699 MeV
			3.0 (3.85)	260 + 2000 M	760 MeV

Proton Acceptance

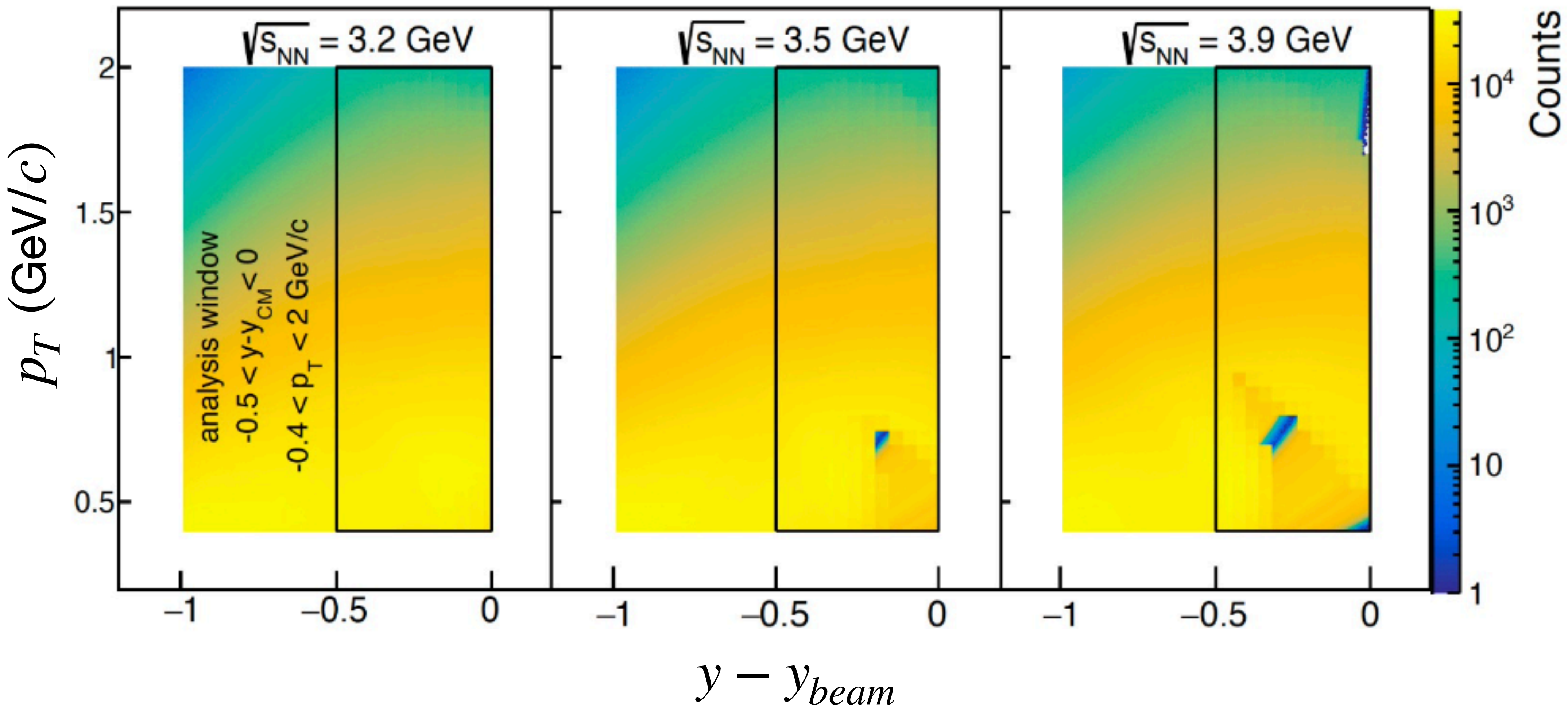

Centrality Definition

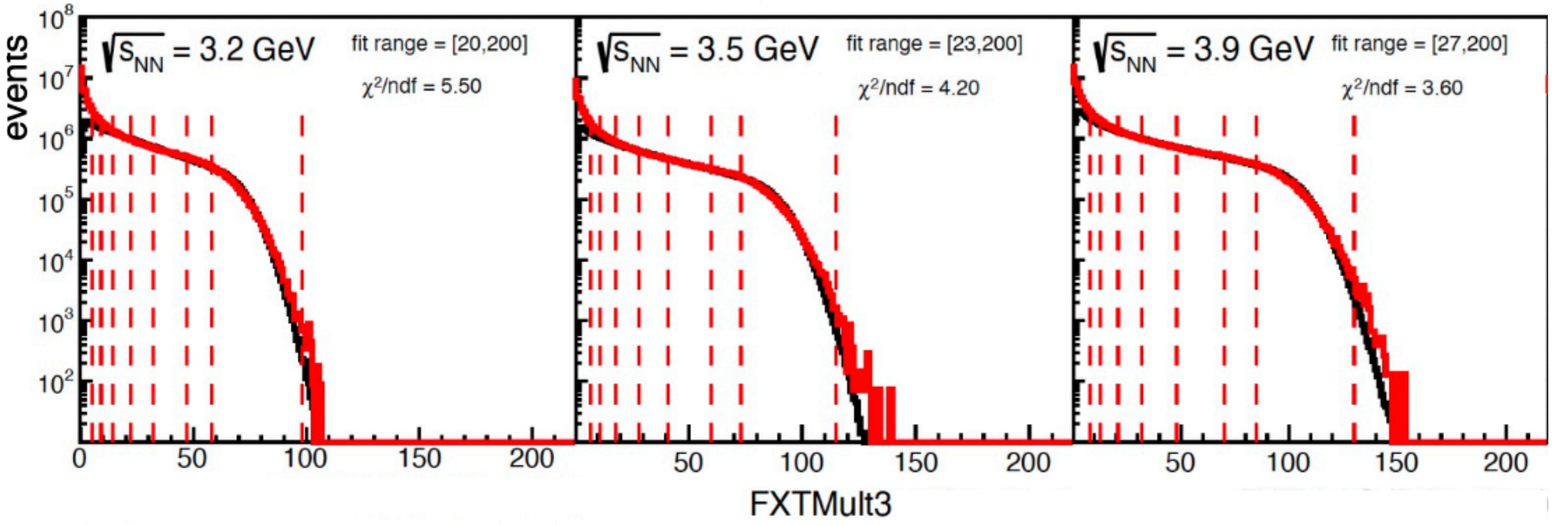

Fluctuation Measures

(Central) Moments $\longleftrightarrow$ **Cumulants** C

$M = C_1,\ \sigma^2 = C_2$

$S = \dfrac{C_3}{(C_2)^{3/2}},\ \kappa = \dfrac{C_4}{C_2^2}$

$\dfrac{C_2}{C_1} = \dfrac{\sigma^2}{M},\ \dfrac{C_3}{C_2} = S\sigma$

$\dfrac{C_4}{C_2} = \kappa\sigma^2$

$C_1 = \langle N \rangle$

$C_2 = \langle (\delta N)^2 \rangle$

$C_3 = \langle (\delta N)^3 \rangle$

$C_4 = \langle (\delta N)^4 \rangle - 3\langle (\delta N)^2 \rangle^2$

Factorial Cumulants κ

$\kappa_1 = C_1$

$\kappa_2 = -C_1 + C_2$

$\kappa_3 = 2C_1 - 3C_2 + C_3$

$\kappa_4 = -6C_1 + 11C_2 - 6C_3 + C_4$

N: Event-by-event multiplicity

$\delta N = N - \langle N \rangle$

- **Cumulants** quantify the shape of distributions / fluctuations;
- **Factorial cumulants** capture genuine multi-particle correlations.

Fluctuation in Proximity to the Critical Point

Cumulants of Conserved Quantities (B, S, Q)

M. Stephanov: PRL 102 032301 (2009)
M. Stephanov: PRL 107 052301 (2011)

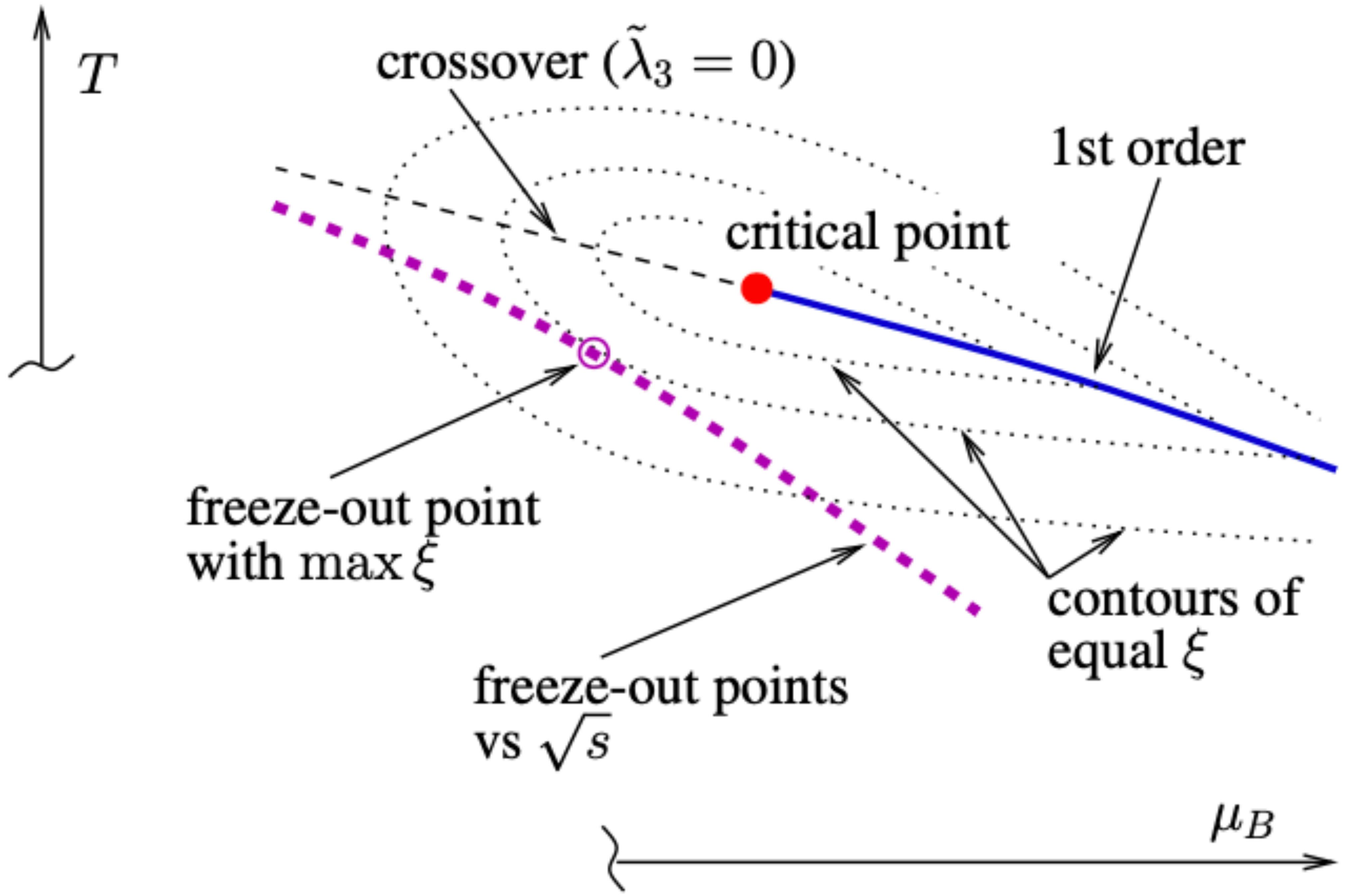

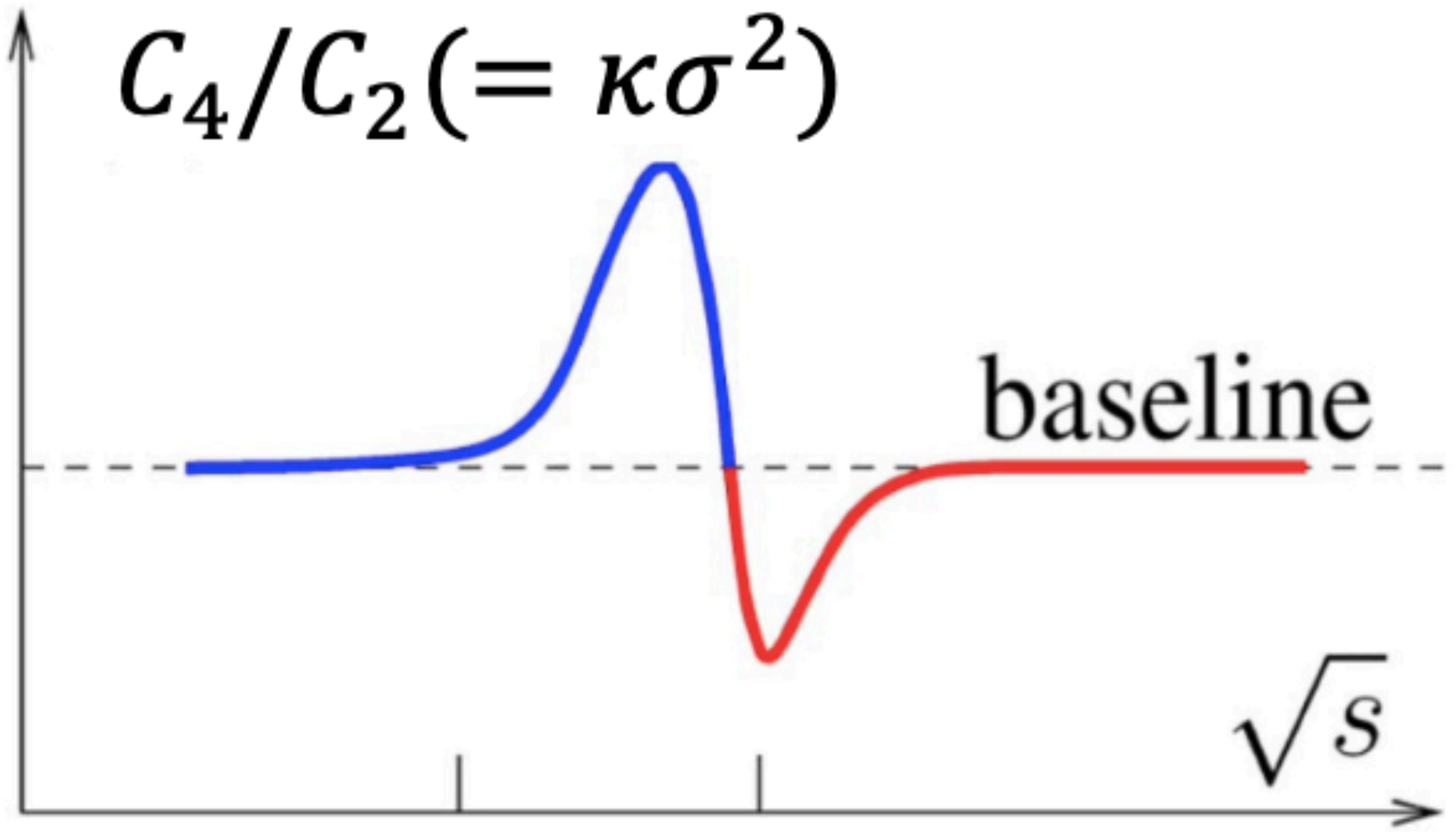

1. Sensitive to correlation length ξ: $C_2 \sim \xi^2$, $C_4 \sim \xi^7$;
2. Directly related to the susceptibility: $\chi_n^{B,S,Q} = C_n^{B,S,Q}/(VT^3)$, $C_4/C_2 = \chi_4/\chi_2$;
3. Non-monotonic energy dependence of C_4/C_2 for the conserved baryon number (using protons as a proxy) indicates the existence of a critical region;
4. Broader energy range and higher statistics in BES-**II** will help reveal clearer signals.

Fluctuation in Proximity to the Critical Point

Hyper Order Cumulants: Diagnostic of the Phase Transition

HotQCD: PRD 101 074502 (2020)
W. Fu, et al: PRD 104 094047 (2021)

$$C_5 = \langle(\delta N)^5\rangle - 5\langle(\delta N)^3\rangle\langle(\delta N)^2\rangle$$
$$C_6 = \langle(\delta N)^6\rangle - 15\langle(\delta N)^4\rangle\langle(\delta N)^2\rangle - 10\langle(\delta N)^3\rangle^2 + 30\langle(\delta N)^2\rangle^3$$
$$\kappa_5 = 24C_1 - 50C_2 + 35C_3 - 10C_4 + C_5$$
$$\kappa_6 = -120C_1 + 274C_2 - 225C_3 + 85C_4 - 15C_5 + C6$$

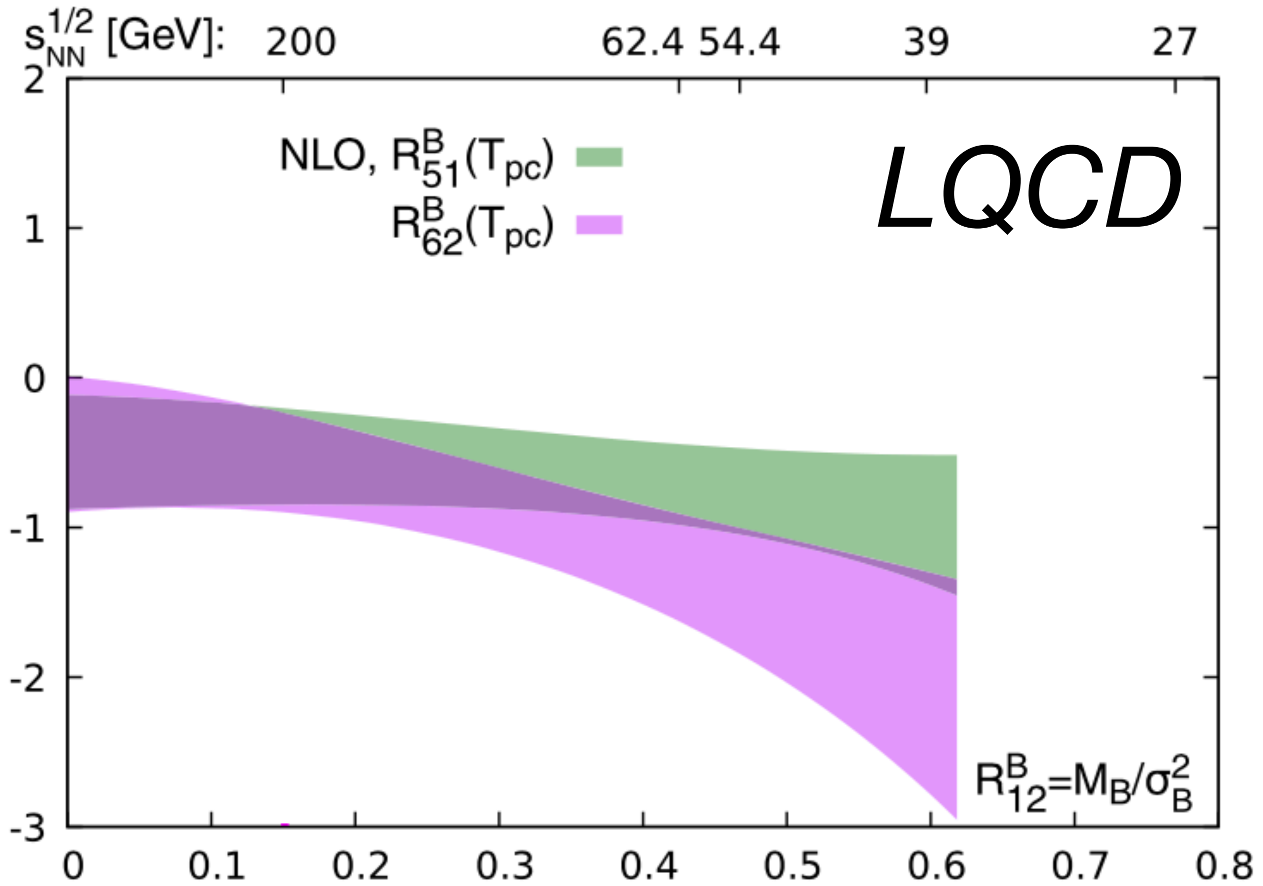

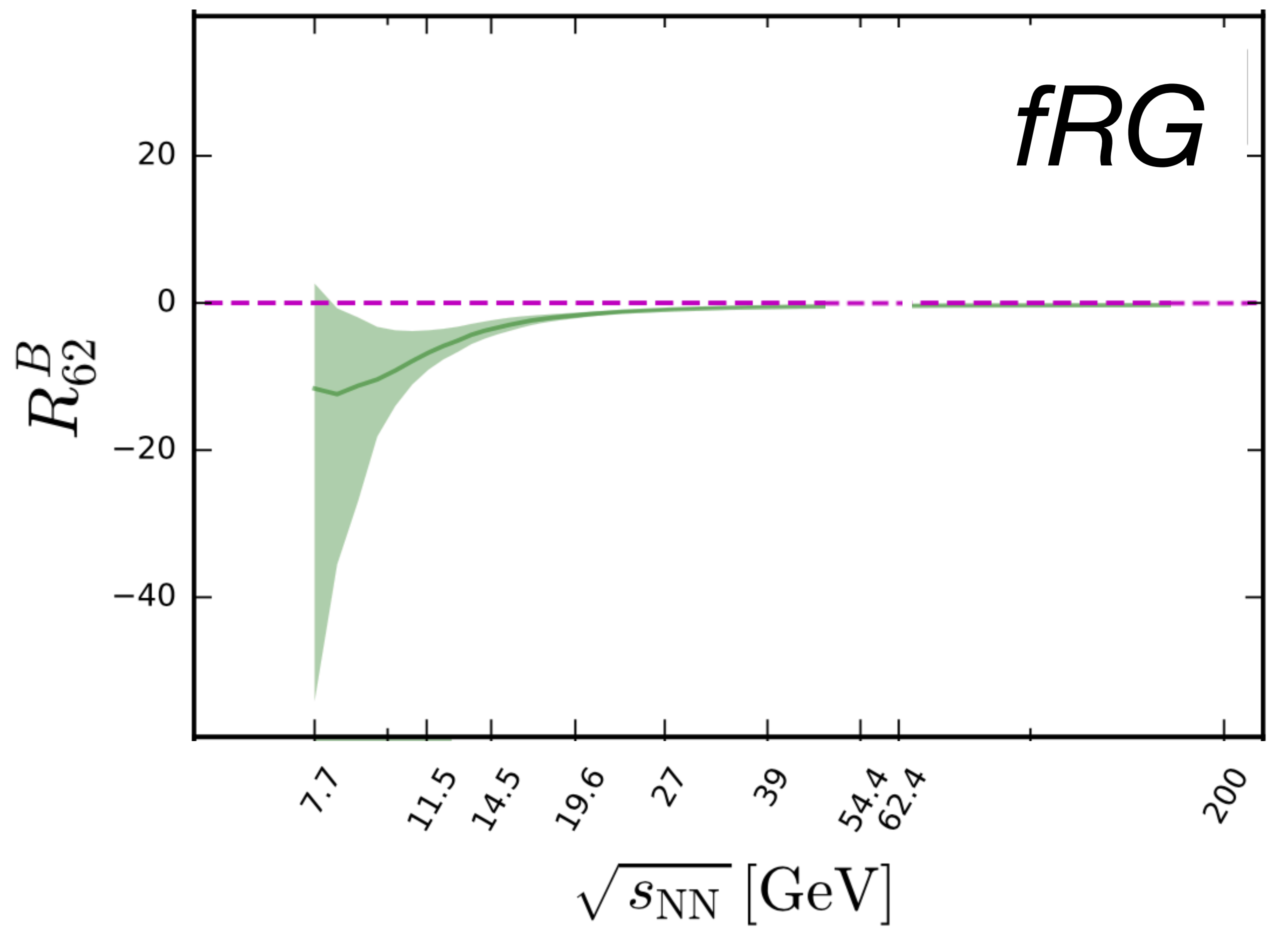

1. Negative C_5/C_1 and C_6/C_2 indicate the smooth crossover nature of the QCD transition;
2. A 7–18 fold increase in statistics in BES-**II** compared to BES-I will reduce uncertainties and improve the reliability of the results.

Fluctuation in Proximity to the Critical Point

B.Ling and M.A.Stephanov: PRC 93 034915 (2016)

Power-law Behavior: Proton Number Factorial Cumulants in Kinematic Scan

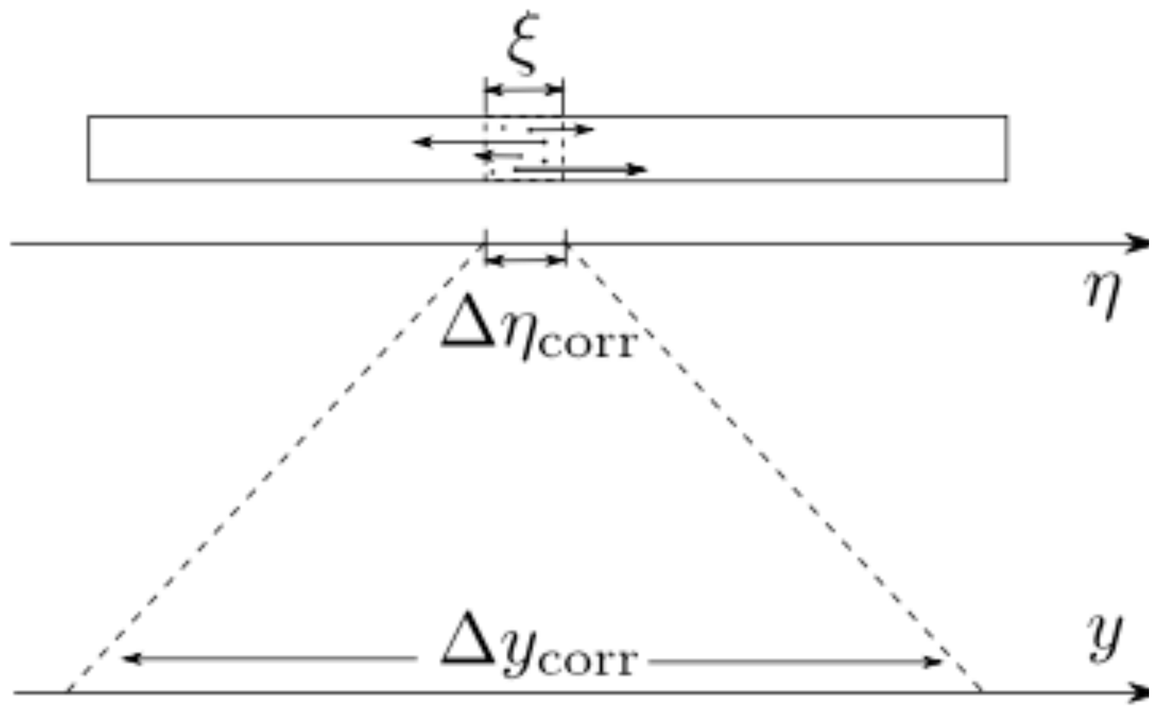

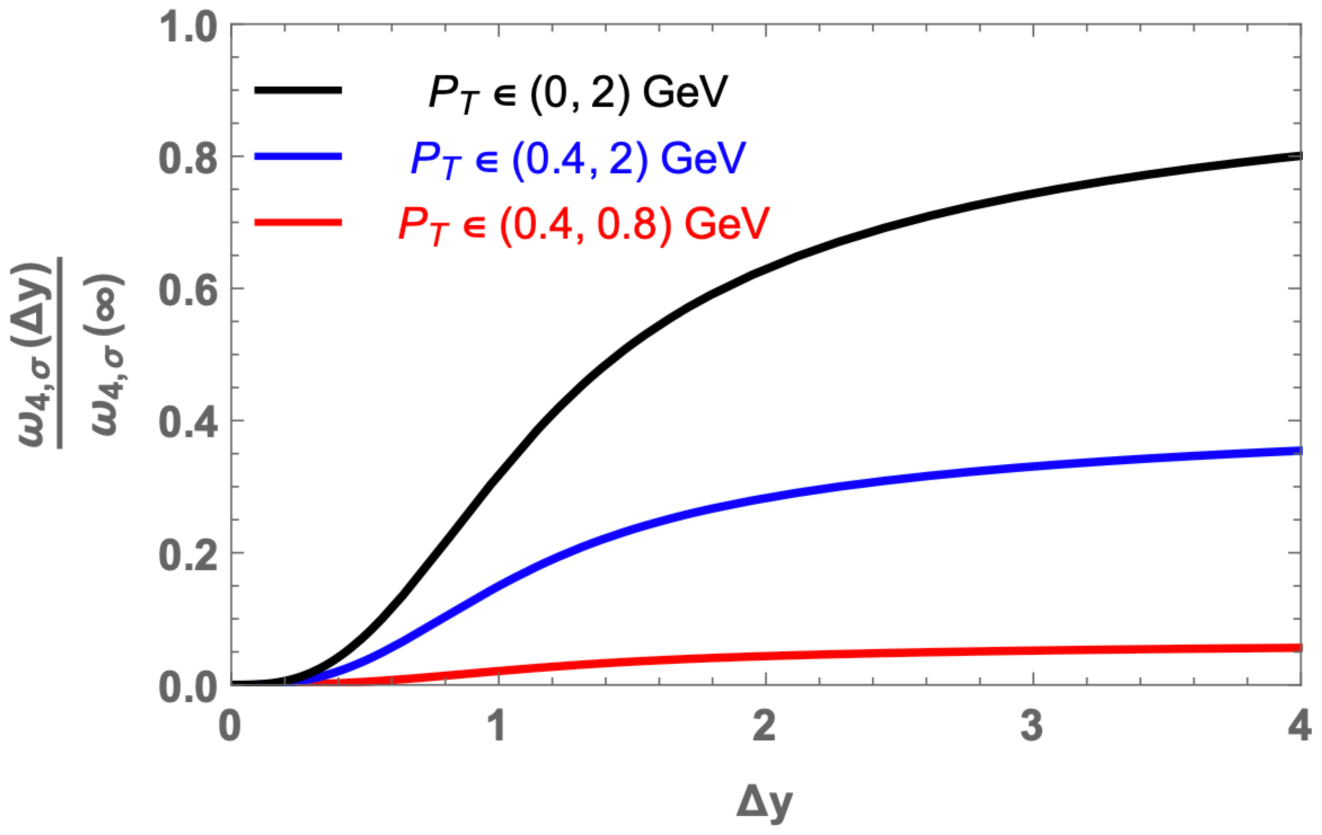

very large Δy_{corr} near the CEP

The opposite, small acceptance regime, $\boxed{\Delta y \ll \Delta y_{\rm corr},}$ is easier to describe using the *factorial* cumulants, $\hat{\kappa}_k$, because they scale as $(\Delta y)^k$ in this regime. The normal cumulants, on the other hand, given by linear combinations of factorial cumulants in Eq. (3), have a more complicated, polynomial dependence on Δy in this regime.

1. Perform a rapidity scan to probe long-range phenomena near the critical point: a wider rapidity window amplifies their contribution;
2. Near the critical point, within small rapidity window $\Delta y \ll \Delta y_{corr}$, we expect $\kappa_n \sim (\Delta y)^n$;
3. BES-**II** offers wide acceptance for long-range studies and high statistics for reliable fits.

Fluctuation in Proximity to the Critical Point

A.Sorensen and P.Sorensen: arXiv:2405.10278[nucl-th]

Extrapolation the critical point via Finite-Size Scaling Method

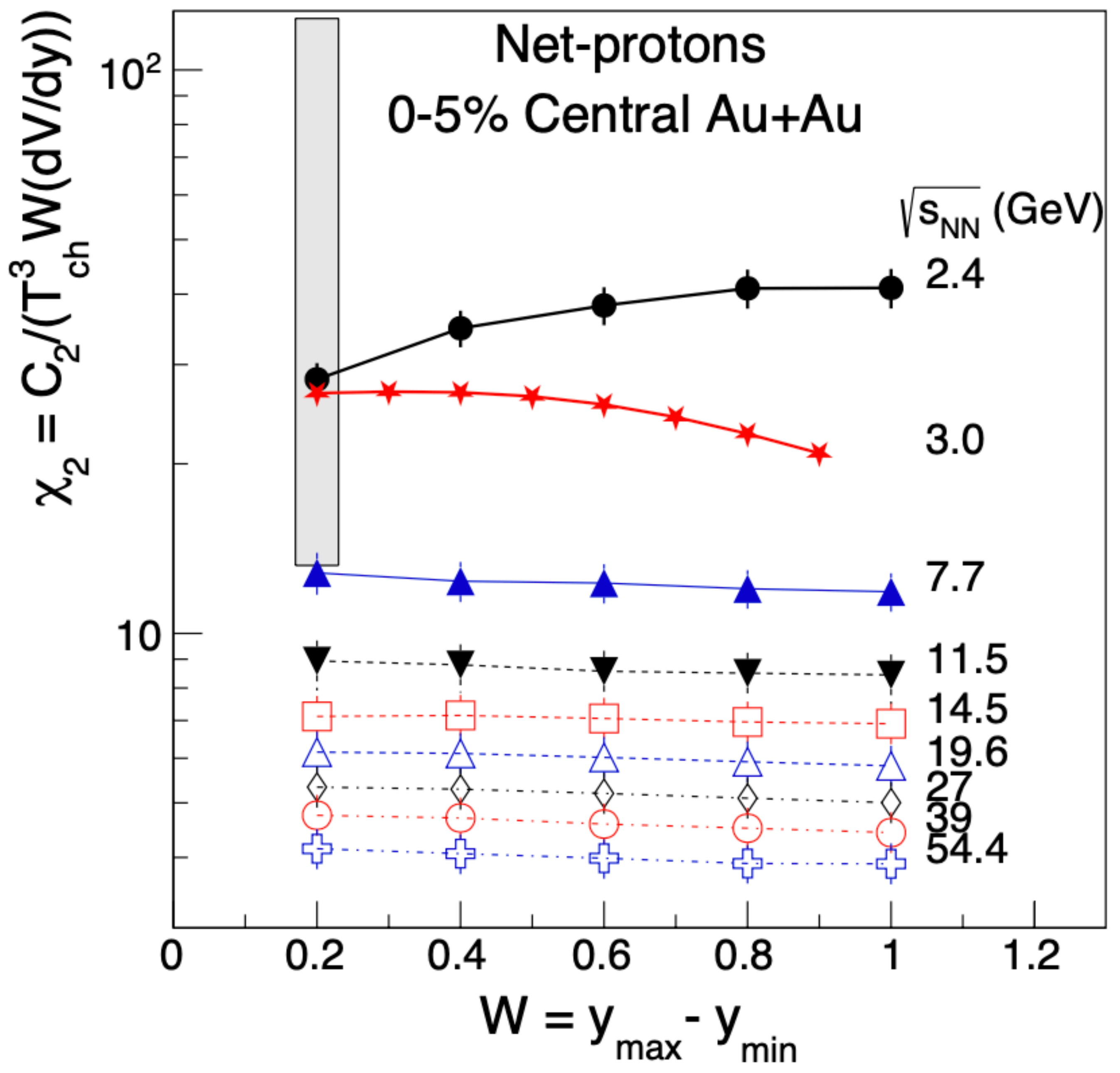

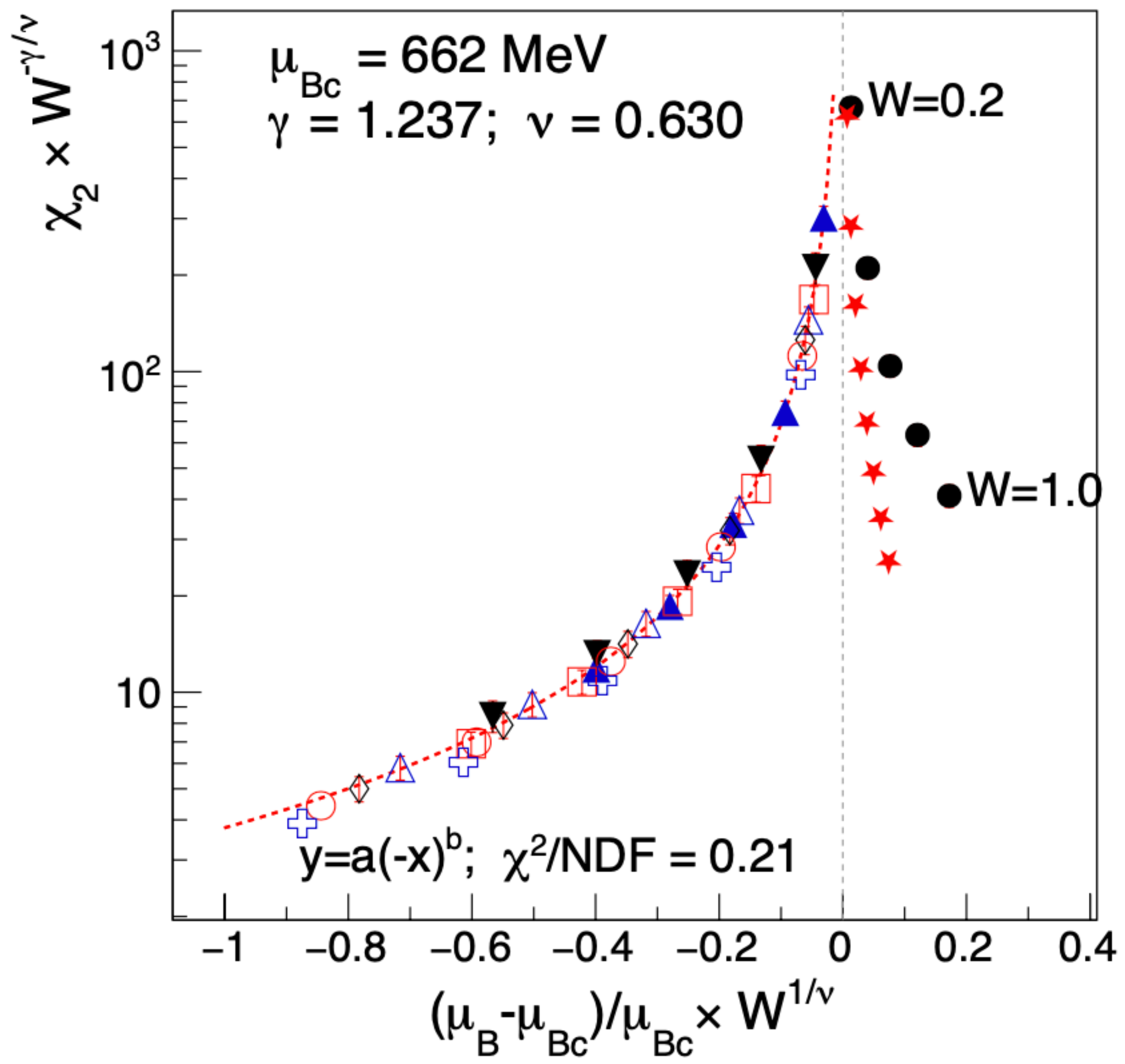

$\nu \approx 0.630$ [42]. Based on Eq. (1), if $\chi L^{-\gamma/\nu}$ is plotted as a function of $tL^{1/\nu}$, then data for different system sizes and values of t should collapse on a single universal curve Φ; the crucial insight for using FSS in finding the critical point is that this can only take place when the correct value of T_c, $\mu_{B,c}$, or $(\frac{\mu_B}{T})_c$ is used in t. Thus, scanning ranges of values of T_c or $\mu_{B,c}$ until the data collapse occurs provides a valuable method to determine the location of a critical point.

$$\chi(L,t) = L^{\gamma/\nu}\Phi(tL^{1/\nu}) \ , \qquad (1)$$

1. Construct susceptibility with measured cumulants and thermal parameters: $\chi_2(W,\mu_{fo}) = \dfrac{C_2(W,\mu_{fo})}{T^3_{fo} W dV_{fo}/dy}$;
2. Finite-Size Scaling analysis requires a proper $\mu_{\rm Bc}$ to exhibit power-law dependence;
3. STAR BES-**II** provides sufficient statistics for a precise extrapolation.

Fluctuation in Proximity to the Critical Point

A.Sorensen and P.Sorensen: arXiv:2405.10278[nucl-th]

Intersection Point of the Binder Cumulant

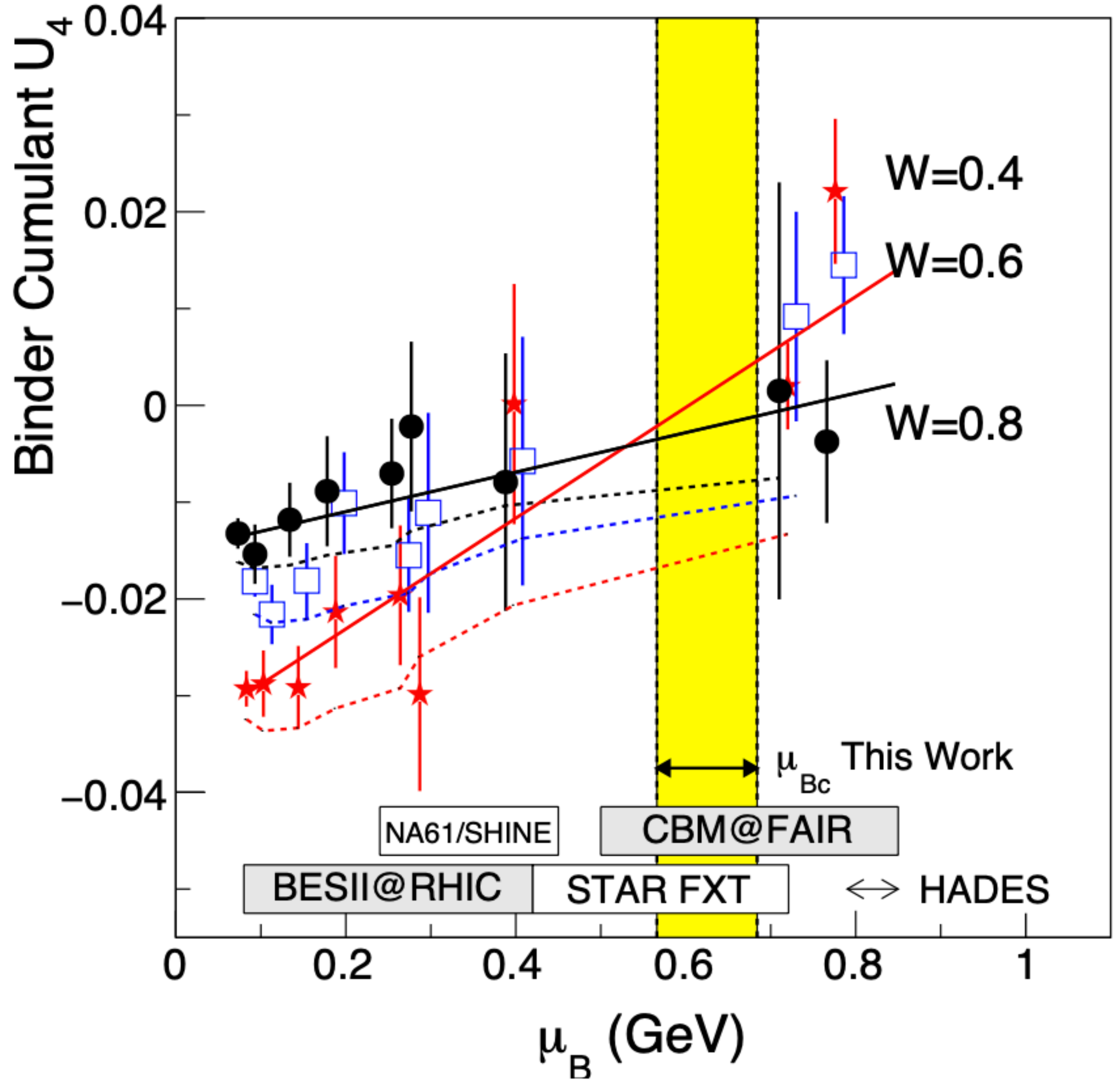

1. $U_4 = -3C_4/C_2^2$;
2. $U_4(\mu_B)$ in different rapidity window (W) is expected to cross at the critical point;
3. An ordering change between left (COL) and right (FXT) is observed in STAR BES-I + STAR FXT 3 GeV + HADES 2.4 GeV Au+Au collisions;
4. High-precision measurements in BES-**II** will provide further insights.

Proton Cumulants @ 3 GeV

STAR: PRL 126 092301 (2021) (BES-I)
STAR: PRL 128 202303 (2022)
STAR: PRC 107 024908 (2023)
HADES: PRC 102 024914 (2020)

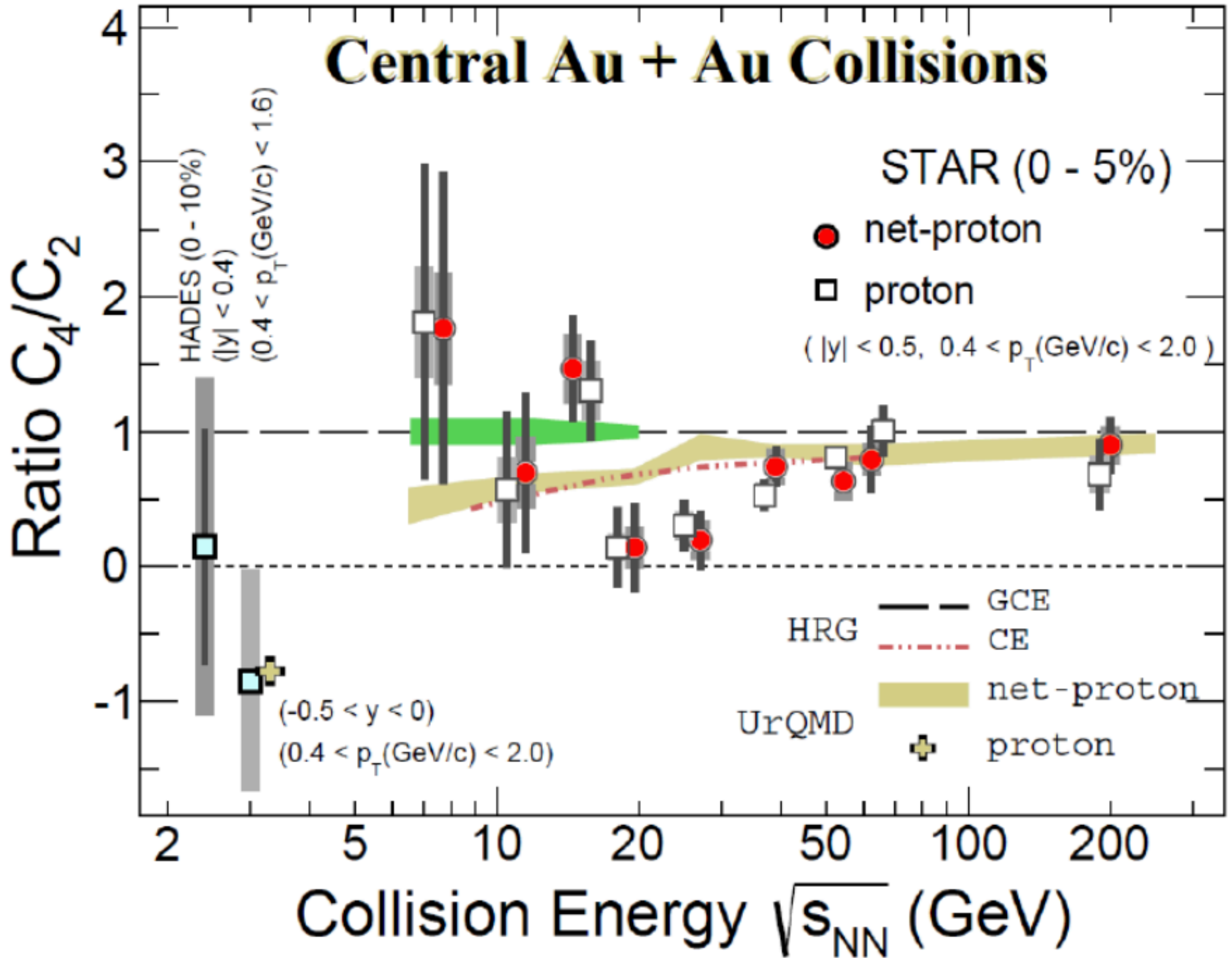

1. STAR's first FXT experiment: to explore the high baryon density region.
2. Well reproduced by UrQMD: dominated by hadronic interactions;
3. Lower energy limit for CEP.

Energy Dependence: BES-II COL Mode

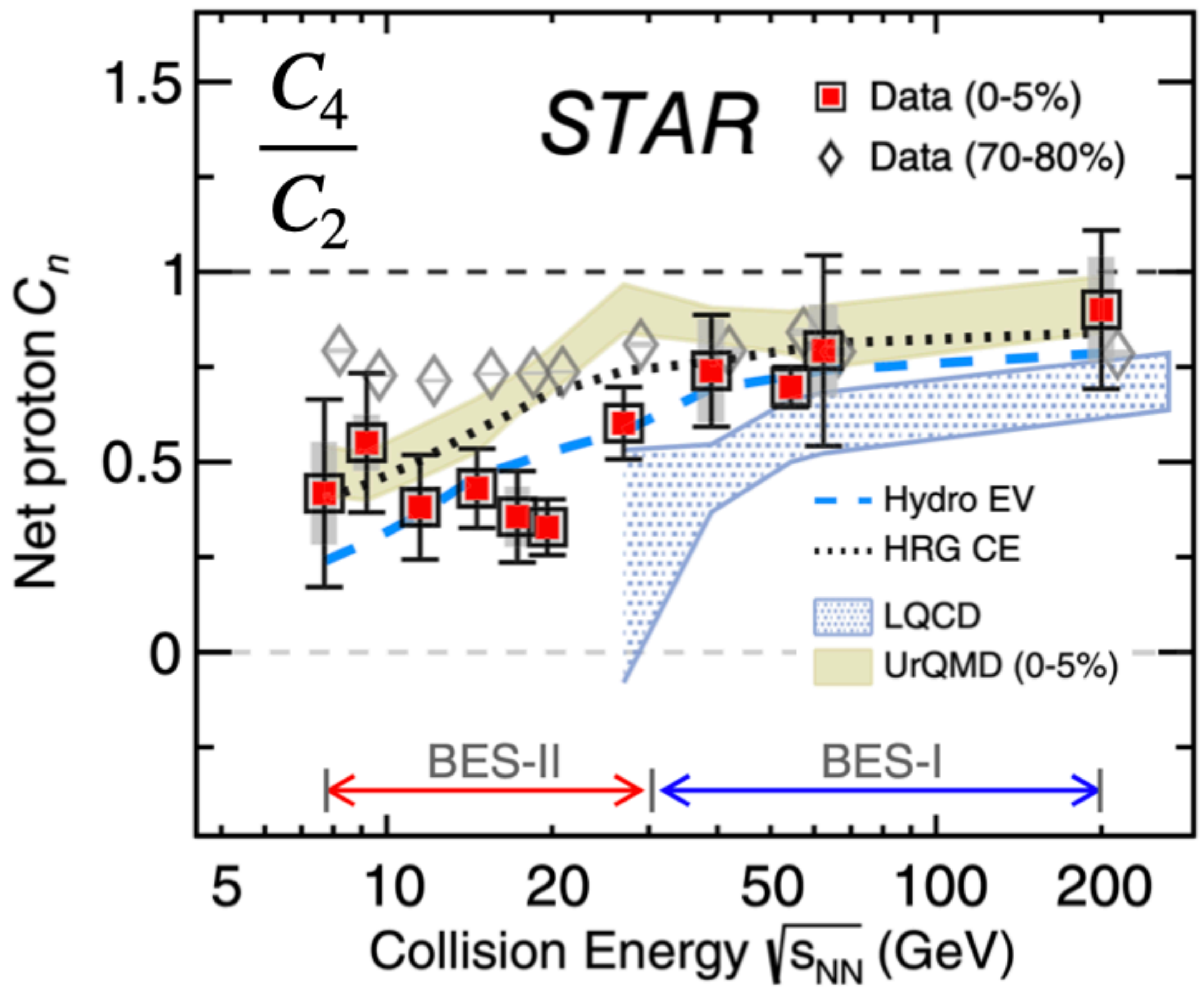

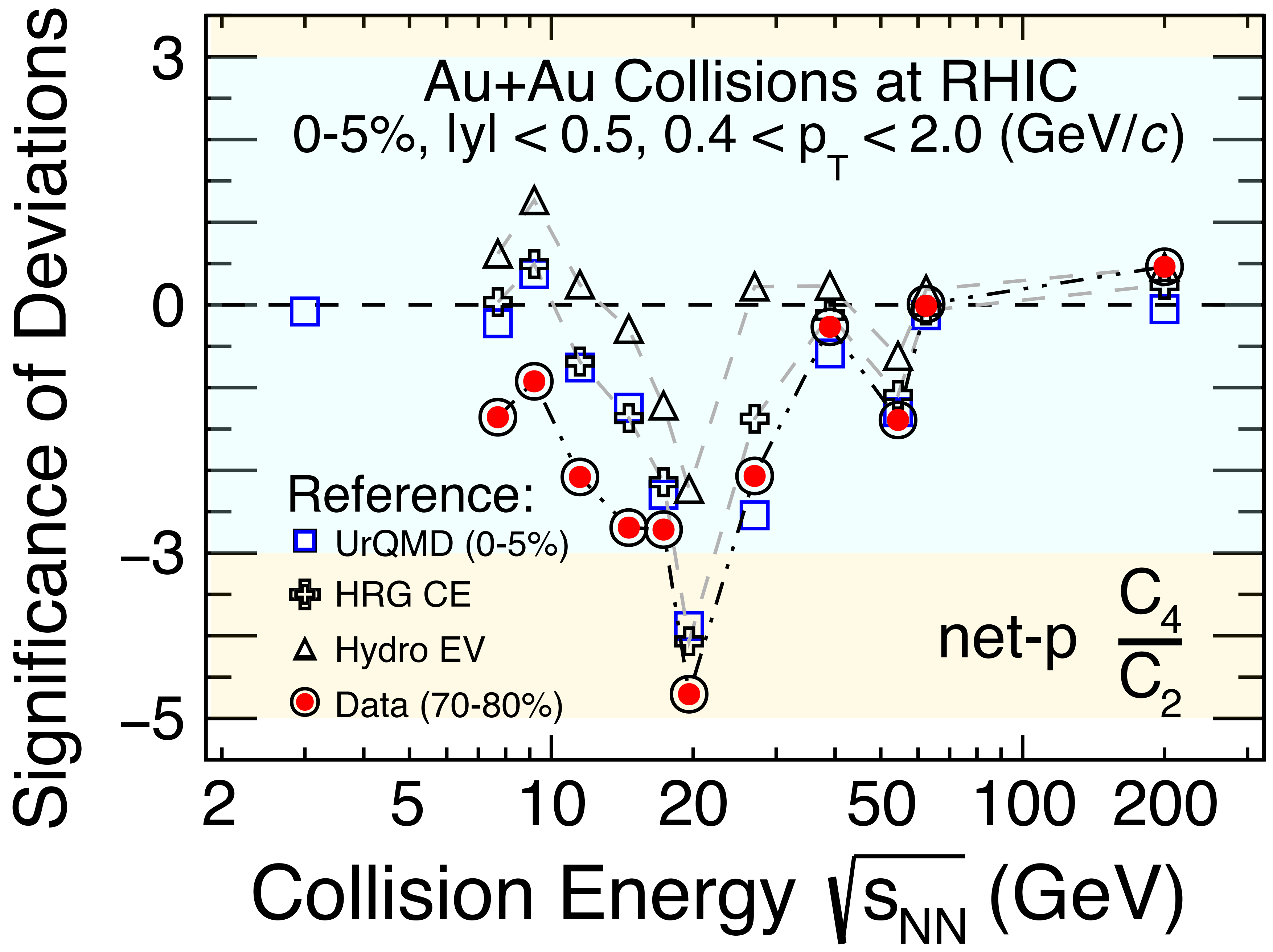

S. Bass, et al: PPNP 41 255 (1998)
P. B. Munzinger, et al: NPA 1008 122141 (2021)
V. Vovchenkov, et al: PRC 105 014904 (2022)
HotQCD: PRD 101 074502 (2020)
STAR: PRL135 142301 (2025)

$$\text{Significance} = \frac{\text{Data} - \text{Ref.}}{\sigma_{total}}$$

Data: STAR 0-5% Result

1. Reduced uncertainty: 4.7 / 3.2 reduction in statistical / systematic errors;
2. Largest negative deviation: 2 – 5σ at $\sqrt{s_{NN}}$=19.6 GeV;

Energy Dependence: BES-II COL Mode

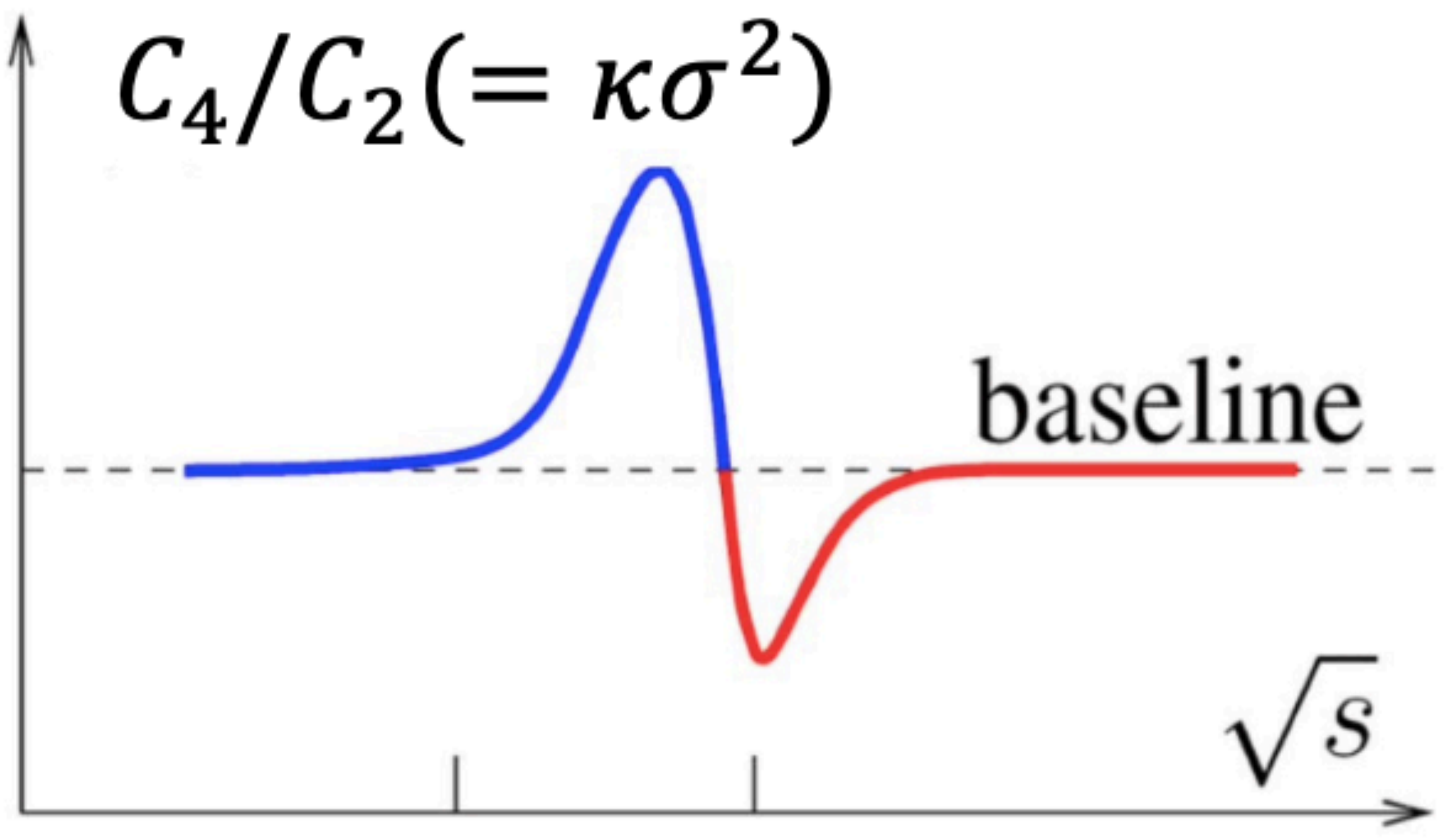

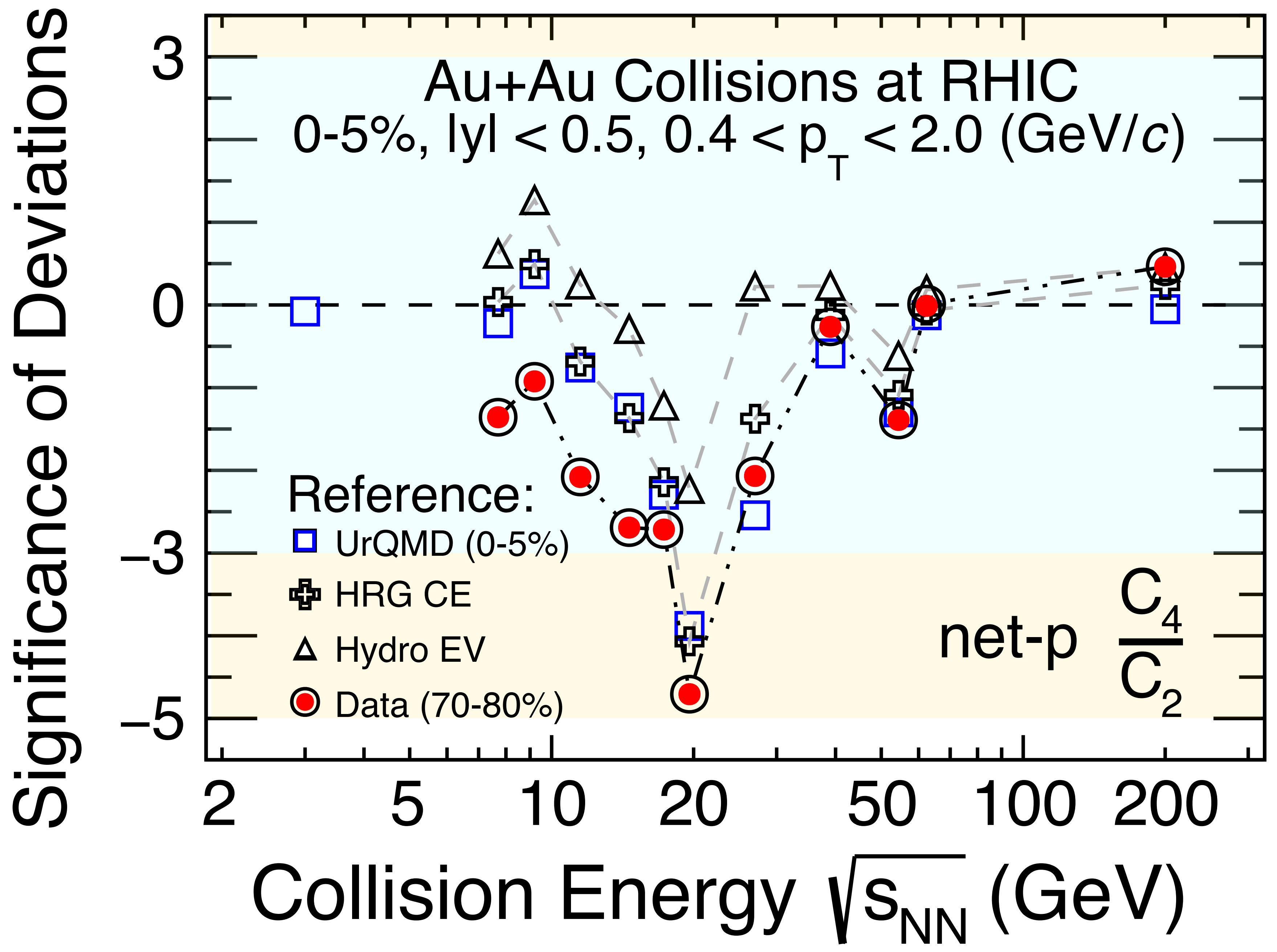

S. Bass, et al: PPNP 41 255 (1998)
P. B. Munzinger, et al: NPA 1008 122141 (2021)
V. Vovchenkov, et al: PRC 105 014904 (2022)
HotQCD: PRD 101 074502 (2020)
STAR: PRL135 142301 (2025)
M. Stephanov: PRL 102 032301 (2009)

$$\text{Significance} = \frac{\text{Data} - \text{Ref.}}{\sigma_{total}}$$

Data: STAR 0-5% Result

1. Reduced uncertainty: 4.7 / 3.2 reduction in statistical / systematic errors;
2. Largest negative deviation: 2 – 5σ at $\sqrt{s_{NN}}$=19.6 GeV;
3. Red valley 😄 blue peak🤔?

Energy Dependence: BES-II FXT Mode

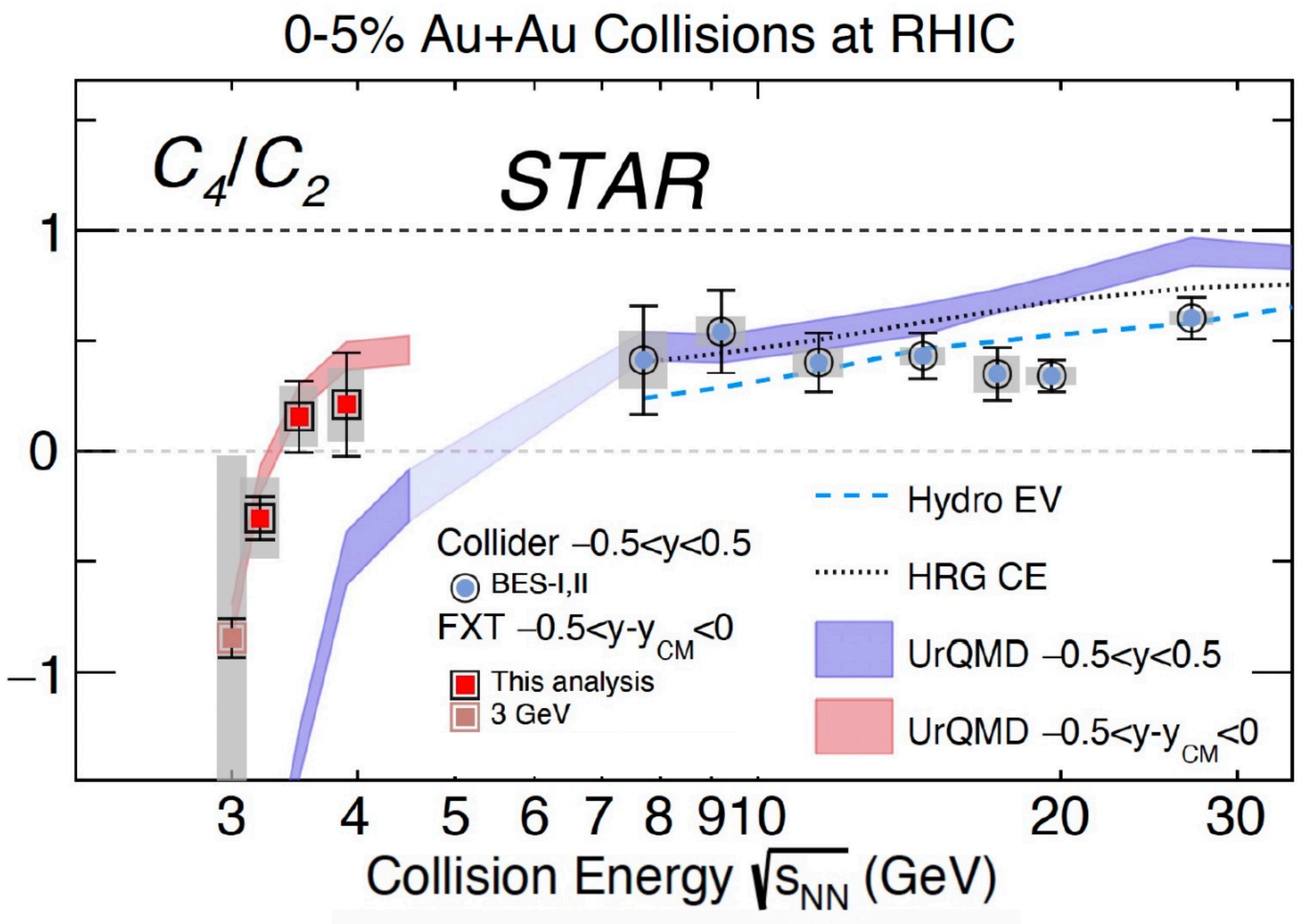

S. Bass, et al: PPNP 41 255 (1998)
P. B. Munzinger, et al: NPA 1008 122141 (2021)
V. Vovchenkov, et al: PRC 105 014904 (2022)
HotQCD: PRD 101 074502 (2020)
STAR: PRL 128 202303 (2022)

Z. Sweger @ QM2025

1. Measurements at $\sqrt{s_{NN}}$=3.2, 3.5 and 3.9 GeV: consistent with UrQMD;
2. Greatly reduced systematic uncertainty: compared with 3 GeV;
3. Important region: experimental results between 4 and 8 GeV;
4. Ongoing work: analyses of 4.5 GeV and high statistics 3 GeV (~2B events).

Energy Dependence: Hyper-Order Results

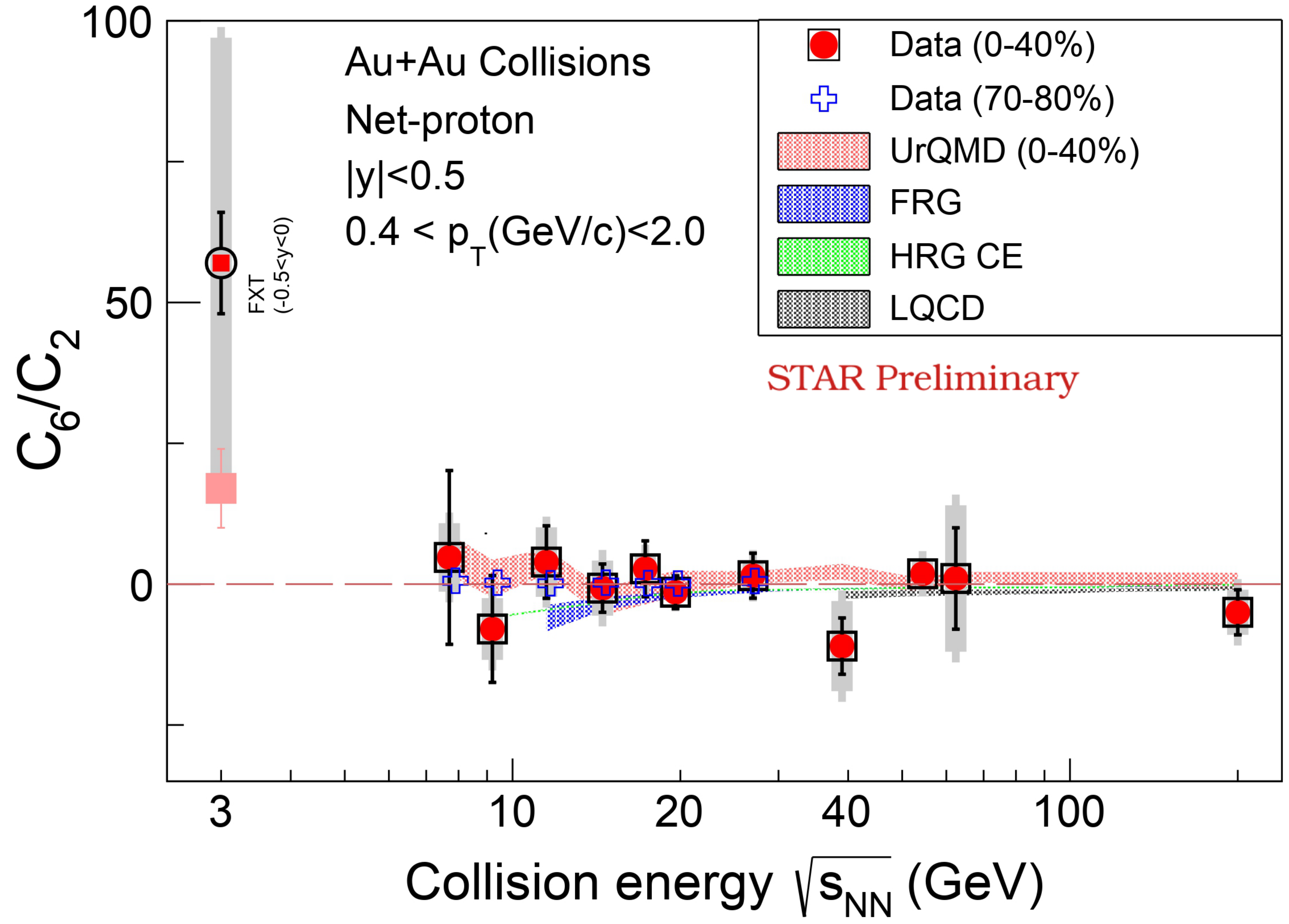

S. Bass, et al: PPNP 41 255 (1998)
P. B. Munzinger, et al: NPA 1008 122141 (2021)
W. Fu, et al: PRD 104 094047 (2021)
HotQCD: PRD 101 074502 (2020)
STAR: PRC 107 024908 (2023)

1. Hyper-order values: fluctuate near zero;
2. Possible indication of a crossover: within 1σ uncertainty, results allow negative value.

B. Mondal @ QM2025

Rapidity Scan: Proton Factorial Cumulants

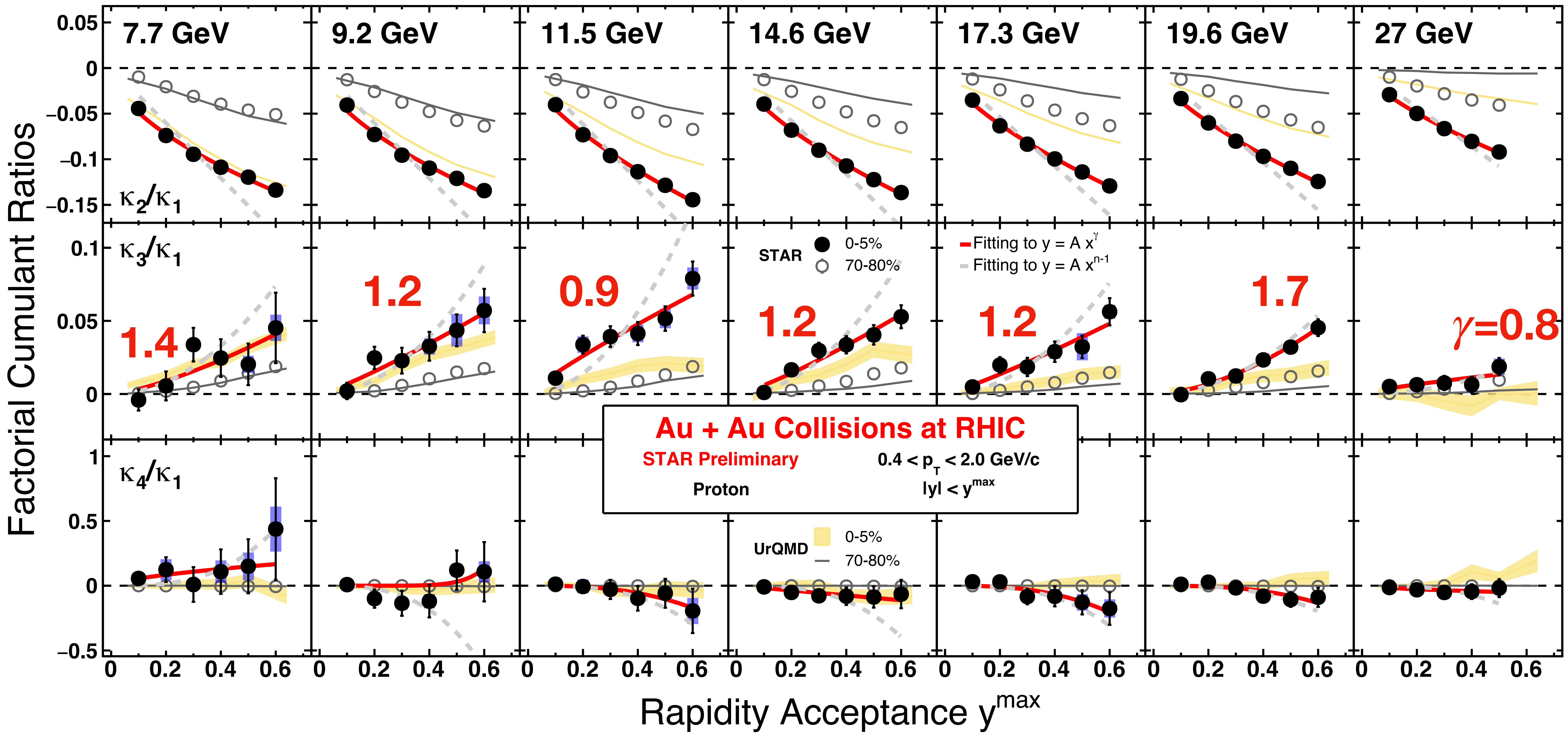

S. Bass, et al: PPNP 41 255 (1998)
B.Ling and M.A.Stephanov: PRC 93 034915 (2016)

Deep red solid curve

(—): Fitting to $y = Ax^{\gamma}$

Light gray dashed curve

(- -): Fitting to $y = Ax^{n-1}$

YH @ QM2025

1. UrQMD agreement: consistent trend, mismatch at high $\sqrt{s_{NN}}$ and large Δy;
2. $\kappa_n/\kappa_1 \sim (\Delta y)^{n-1}$: power-law behavior observed with smaller exponents.

Extrapolating the CEP: Finite-Size Scaling

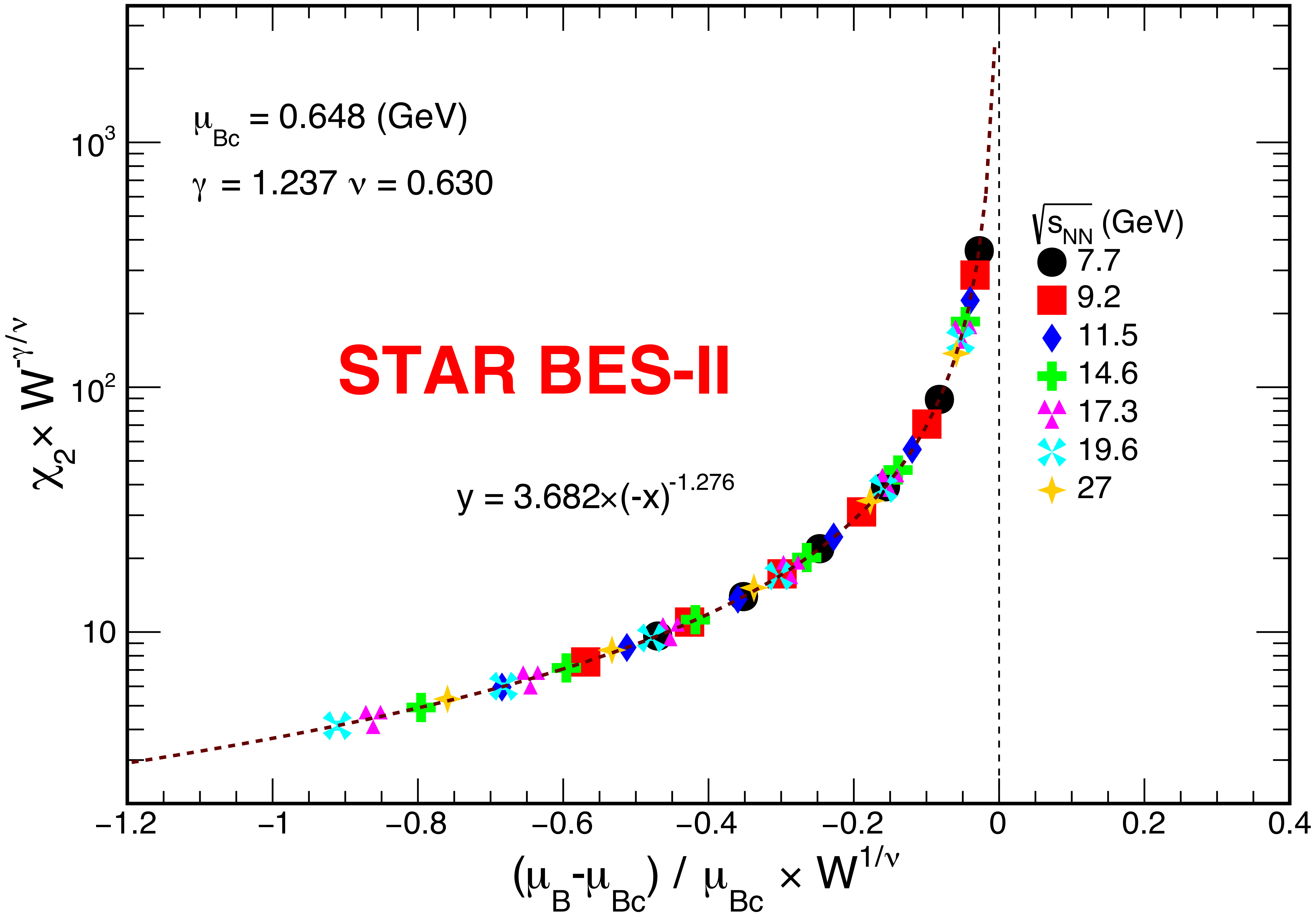

A.Sorensen and P.Sorensen: arXiv:2405.10278[nucl-th]
A.Andronic, et al: Nature 561 7723 321-330 (2018)
J.V.Sengers and J.G.Shanks: Journal of Statistical Physics 137 857 (2009)

YH @ QM2025

1. Consistent results, with significantly reduced fit uncertainty: $\mu_{Bc} = 648^{+4}_{-3}$ MeV v.s. 662^{+22}_{-20} MeV;
2. Critical μ_B range: 590 — 652 MeV with combined fit and systematic uncertainty.

Ordering Change of Binder Cumulant

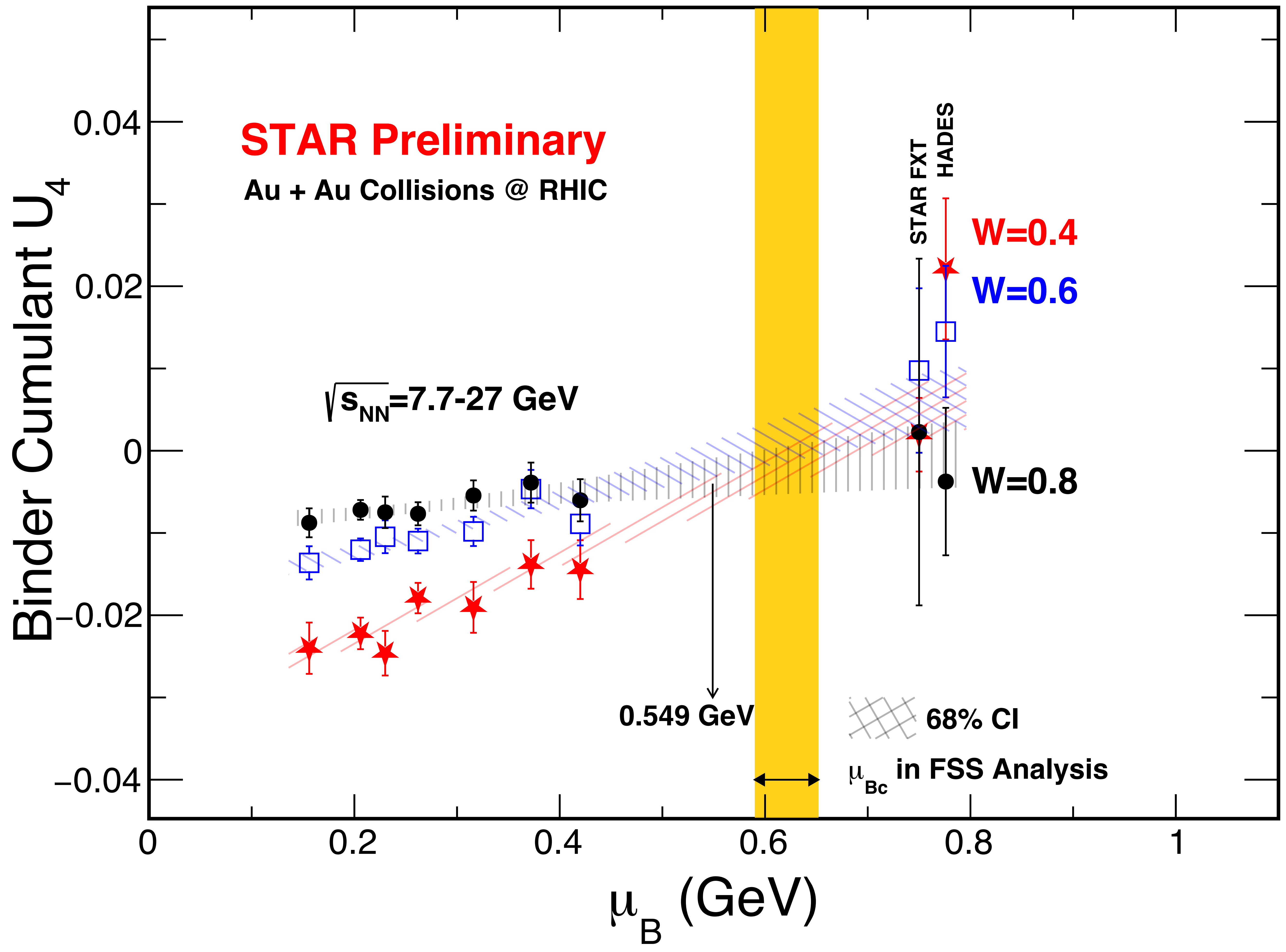

A.Sorensen and P.Sorensen: arXiv:2405.10278[nucl-th]
STAR: STAR: PRC 107 024908 (2023)
HADES: HADES: PRC 102 024914 (2020)

YH @ QM2025

1. Reversed ordering with μ_B: black > blue > red (left), red > blue > black (right);
2. Shaded bands show linear fits with 68% C.I.: overlapping starts at μ_B = 549 MeV.

Summary

1. STAR reported precision measurements of (net-)proton fluctuations in Au+Au collisions at 3.0 — 3.9 GeV (FXT) and 7.7 — 27 GeV (COL).
   - With better statistics, control on systematics, and centrality resolution.
2. Collider Energies:
   1. Net-proton C_4/C_2 shows largest deviation w.r.t non-CP baselines at 19.6 GeV with 2 — 5σ;
   2. Hyper-order cumulants indicate smooth crossover in the energy range 7.7 — 27 GeV;
   3. Rapidity scan of (net-)proton fluctuations suggests the CEP may lie at higher baryon densities, possibly in a μ_B range 550 — 650 MeV.
3. Fixed-target Energies:
   1. Proton C_4/C_2 are consistent with UrQMD in the energy range 3.0 — 3.9 GeV;
   2. Analysis of 4.5 GeV and high statistics 3 GeV (~2B events) are underway.

Outlook

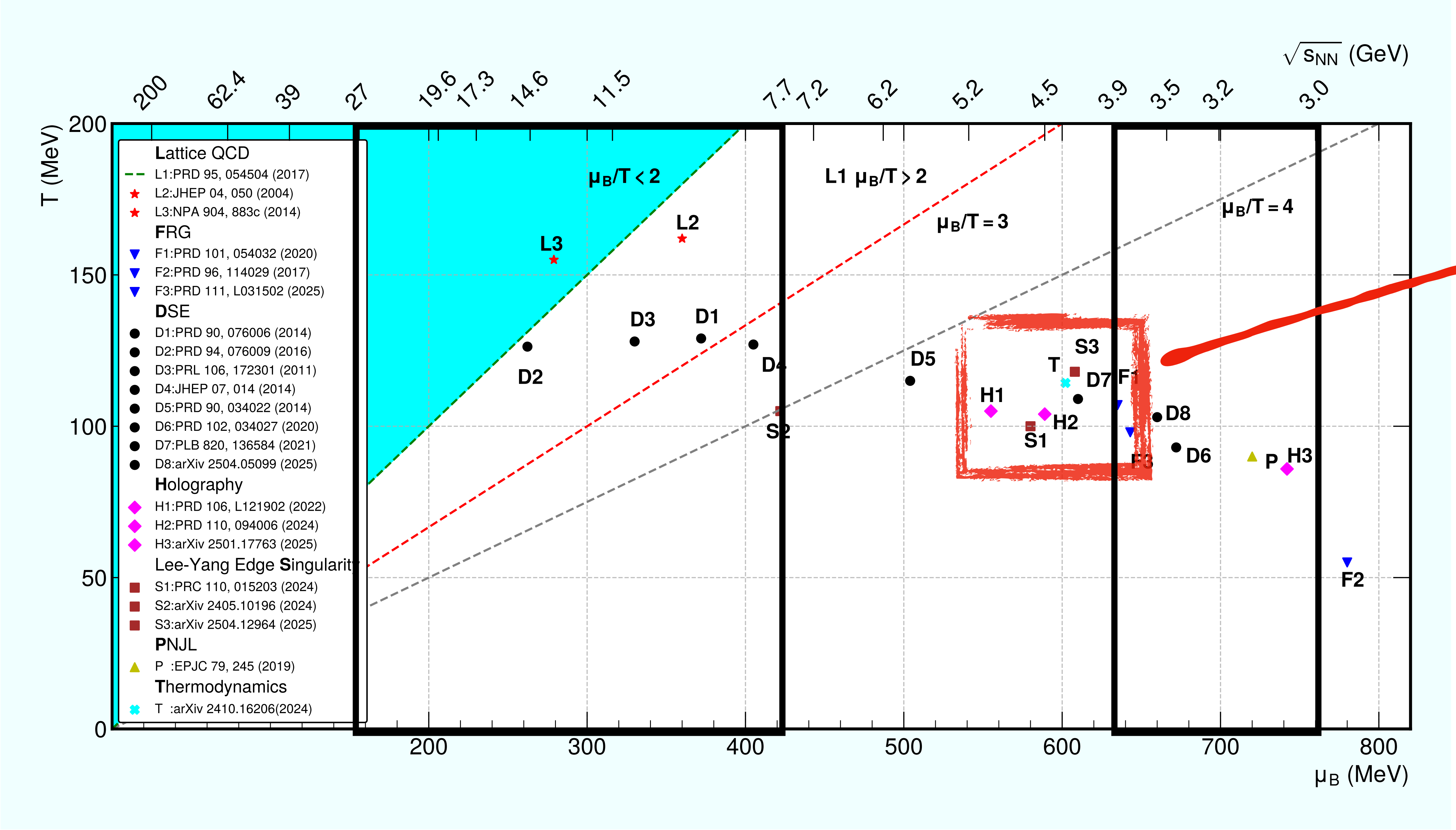

Thank you for your attention!

Experiments focusing on physics at high baryon density:

- China: CEE
- Germany: CBM
- USA: STAR (FXT)
- Russia: MPD

...